Science of the Total Environment 798 (2021) 149310

Contents lists available at ScienceDirect

Science of the Total Environment

journal homepage: www.elsevier.com/locate/scitotenv

High contribution of vehicle emissions to fine particulate pollutions in Lanzhou, Northwest China based on high-resolution online data source appointment

Min Wang [a], Pengfei Tian [a,*], Ligong Wang [a], Zeren Yu [a], Tao Du [a], Qiang Chen [a], Xu Guan [a], Yumin Guo [a], Min Zhang [a], Chenguang Tang [a], Yi Chang [c], Jinsen Shi [a,b], Jiening Liang [a], Xianjie Cao [a], Lei Zhang [a,b]

[a] Key Laboratory for Semi-Arid Climate Change of the Ministry of Education, College of Atmospheric Sciences, Lanzhou University, Lanzhou 730000, China
[b] Collaborative Innovation Center for Western Ecological Safety, Lanzhou University, Lanzhou 730000, China
[c] Gansu Province Environmental Monitoring Center, Lanzhou 730020, China

HIGHLIGHTS

- Vehicle emissions were the largest source of particulate matter (PM) pollution.
- Contribution of vehicle emissions increased with increasing PM in winter and autumn.
- Vehicle emissions contributed most to the elemental carbon.

GRAPHICAL ABSTRACT

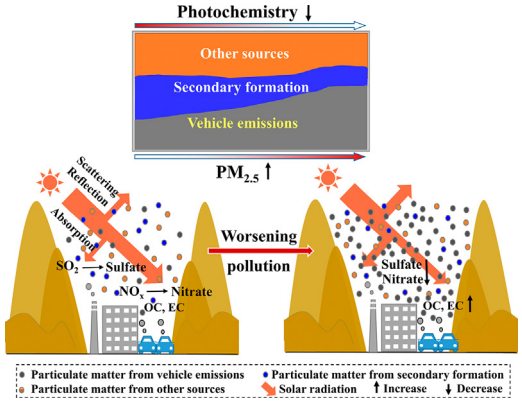

ARTICLE INFO

Article history:
Received 30 June 2021
Received in revised form 20 July 2021
Accepted 23 July 2021
Available online 29 July 2021

Editor: Pavlos Kassomenos

Keywords:
Particulate pollution
Online chemical species
Elemental carbon
Source appointment
Vehicle emissions

ABSTRACT

The quantitative estimation of urban particulate matter (PM) sources is essential but limited because of various reasons. The hourly online data of $PM_{2.5}$, organic carbon (OC), elemental carbon (EC), water-soluble ions, and elements from December 2019 to November 2020 was used to conduct PM source appointment, with an emphasis on the contribution of vehicle emissions to fine PM pollution in downtown Lanzhou, Northwest China. Vehicle emissions, secondary formation, mineral dust, and coal combustion were found to be the major PM sources using the positive matrix factorization model. The seasonal mean $PM_{2.5}$ were estimated to be 72.8, 39.2, 24.3, and 43.6 $\mu g \cdot m^{-3}$ and vehicle emissions accounted for 35.7%, 25.8%, 30.0%, and 56.6% in winter, spring, summer, and autumn, respectively. Vehicle emissions were the largest source of PM considering the high PM pollution in winter and its significantly large contribution in autumn. Furthermore, the contribution of vehicle emissions increased with increasing PM in winter and autumn. Vehicle emissions were also the most important source of EC, accounting for 70.3%, 91.0%, 83.5%, and 93.7% of the total EC in winter, spring, summer, and autumn, respectively. With the reduction in industrial emissions and increase in vehicle numbers in China in recent years, vehicle emissions are going to be the largest source of urban PM pollution. To sustainably improve air quality in Lanzhou and other Chinese cities, efforts should be made to control vehicle emissions such as promoting clean-energy vehicles and encouraging public transportation.

* Corresponding author.
E-mail address: tianpf@lzu.edu.cn (P. Tian).

https://doi.org/10.1016/j.scitotenv.2021.149310
0048-9697/

1. Introduction

Cities worldwide have been suffering from high loading of atmospheric particulate matter (PM) pollutants originating from anthropogenic and natural sources (Daellenbach et al., 2020; Jain et al., 2020). These sources contribute to urban PM pollution through primary emissions and secondary formation in the atmosphere (Zhang et al., 2015; An et al., 2019). The urban PM pollution affects urban environment, influences weather and climate, and damages human health (Venkataraman et al., 2005; Lelieveld et al., 2015). Studies have revealed that these effects vary with PM sources and species (Kim et al., 2015; Tian et al., 2018). Thus, quantitative estimation of the contribution of PM sources is essential but has been limited because of the relative contribution of the sources and the temporal and spatial variations exhibited by them (Barraza et al., 2017; Zhu et al., 2018).

PM sources have always continuously changed because of the development of society and economy and the transformations seen in production and lifestyle. Industrial emissions have declined in the last few decades while vehicle emissions have increased because of increasing number of motor vehicles in cities globally (Chen et al., 2019; Du et al., 2020). Other PM sources include coal combustion in power plant (Wang et al., 2020), mineral dust from natural dust events (floating dust, blown dust, and dust storms) and anthropogenic activities (construction, agriculture, and road dusts), and PM pollutants emitted from festival celebration, such as fireworks from Spring Festival of China (Ji et al., 2018). In addition to primary emissions, gaseous precursors from different sources also contribute to PM pollution by secondary formation in the atmosphere (Huang et al., 2014a). PM pollution in Chinese cities have been significantly improved since the formulation of the Clean Air Plan in China (Chen et al., 2017; Zhang et al., 2019). Meanwhile, the contribution of sources to PM and even source profiles have significantly changed (Zhu et al., 2018; Bi et al., 2019). Therefore, there is an urgent need for the source appointment of PM pollution at present.

Vehicle emissions (also traffic or transport emissions) have already become the largest PM source in many cities, especially in the developed countries such as Kozani, Greece (Toils et al., 2014), Monterrey Metropolitan, Mexico (Martínez-Cinco et al., 2016), and Los Angeles, United States of America (USA) (Sowlat et al., 2016). Vehicle emissions were found to be the second largest source of PM in some Chinese cities (Huang et al., 2017; Liu et al., 2017; Zong et al., 2018). Vehicles directly emit organic carbon (OC), elemental carbon (EC), CO, NOx, CO_2 and NH_3, cause road dust, and lead to the secondary formation of PM pollutants in the atmosphere (Resitoglu et al., 2015). Vehicle emissions are a major source of urban EC and have been used as a tracer for urban vehicle emissions (Huang et al., 2014b; Wong et al., 2020). Specifically, vehicle emissions accounted for 51.9% of the total EC in Beijing, China during 2016–2017 (Cui et al., 2021) and ~ 55.0% in the cities in the USA and Europe (Briggs and Long, 2016). The fraction of EC to fine PM pollutants in a city in Northwest China (Lanzhou) was the highest under high PM pollution conditions when the winter samples were grouped into low, moderate, and high pollution levels (Du et al., 2020), which was opposite to the trends in eastern Chinese cities where the fraction of secondary inorganic aerosols rapidly increased under heavy pollutions (Wang et al., 2016a). Furthermore, the absorption coefficient (mainly caused by carbonaceous aerosols) in Lanzhou was also relatively high among the cities globally at present (Guan et al., 2021). Thus, it is important to quantitatively estimate PM pollution, especially EC, from vehicle emissions in Northwest China.

Positive matrix factorization (PMF) is a widely used receptor model for estimating the sources of PM pollution (Saraga et al., 2019; Zhang et al., 2020; Bie et al., 2021). Aerosol species from offline filter samples have been generally used to run the PMF model (Lee et al., 2008; Tao et al., 2014), the findings of which are an important guide for effectively controlling local PM pollution. However, offline samples usually have a long cycle time for collection and analysis. Thus, results from offline samples always have a time resolution of 12 or 24 h that does not reflect the diurnal variations in the PM sources. Results from these samples are also not applicable in analyzing the PM sources in short-term pollution events immediately. The long-time span of collection and analysis can cause PM sources to change during the study period, which will also violate the assumptions made in the PMF model (Wang et al., 2018). The online monitoring technology of PM species has rapidly developed in recent years. Source appointment using the online data has shown greater advantages in terms of obtaining more robust source analysis results and detailed information about the diurnal variations of the PM sources, as well as providing the opportunity to analyze short-term pollution events immediately after these events. Studies have revealed that results from the high time-resolution online data-based source appointment were more effective and robust than traditional low time resolution ones (Yu et al., 2019).

PM pollution has significantly improved in the recent three decades because of the strict control measures of the government in Lanzhou, which used to be one of the most polluted cities worldwide (Qian et al., 2001). However, PM pollution remains relatively high in Lanzhou when the diffusion conditions are unfavorable, especially in winter when boundary layer height was very low (Du et al., 2020; Zhang et al., 2021). PM sources in Lanzhou have been studied using the PMF model based on offline filter samples, for example, Qiu et al. (2016) examined PM sources at three sites in 2012 using 60 samples per site, Tan et al. (2017) used 68 filter samples collected during winter 2012 and summer 2013, and Wang et al. (2016b) used 84 filter samples collected in 2014. These three studies used daily offline samples with relatively small sample numbers, which lacked the information on diurnal changes in the sources, delayed the result analysis cycle, and provided less credible PMF results. Thus, the urban PM sources in Northwest China have been poorly studied and the changes in PM sources in Lanzhou are unclear since the implementation of the Clean Air Plan in China in 2013. Furthermore, vehicle numbers have rapidly increased in Lanzhou in recent years, from 614,800 at the end of 2014 to 1,144,900 by the end of 2020 (http://tjj.lanzhou.gov.cn/), which may seriously impact PM pollutants, especially the carbonaceous species. Therefore, the high-resolution online data was used to conduct PM source appointment from December 2019 to November 2020, with an emphasis on the contribution of vehicle emissions to fine PM pollution in Lanzhou.

2. Observation site, data, and methodology

2.1. Observation site

Field measurements were conducted from 1 December 2019 to 30 November 2020 at the Lanzhou Atmospheric Components Monitoring Superstation (LACMS; 36.05°N, 103.87°E, 1520 m a.s.l.; Fig. 1), located in the campus of Lanzhou University. To have a better representation on city scale, the instruments at this site were positioned on the roof of a 10-story building (approximately 20 m above the ground) rather than at the ground. Tianshui and West Donggang highways are located to the west and north of the LACMS site, respectively. Xigu district located in the western of the site is the largest petrochemical base of western China. The duration from December 2019 to February 2020 was defined as winter, March to May 2020 as spring, June to August 2020 as summer, and September to November 2020 as autumn. Introductions of the LACMS site and the instreuments are available elsewhere (Du et al., 2020; Guan et al., 2021).

2.2. Instruments and data

A PM synchronous mixing monitor (5030i SHARP, Thermo Fisher, USA) was used to monitor the hourly mass concentrations of PM with an aerodynamic diameter of up to 1.0 μm (PM_1), 2.5 μm ($PM_{2.5}$), 10 μm (PM_{10}), and total suspended particles with a flow rate of

Fig. 1. Site and instruments: (a) topography of Lanzhou; (b) site and surroundings; (c) PM mass concentration monitor; (d) monitor for water-soluble inorganic ions; (e) heavy metal monitor; (f) meteorological sensor; (g) OC/EC monitor; (h) traffic on the Tianshui highway during the evening rush hours.

1 $m^3\ h^{-1}$. A Monitor for AeRosols and Gases in ambient Air (MARGA, Applikon, The Netherlands) was used to measure the hourly water-soluble inorganic ions (WSIIs; Cl^-, NO_3^-, SO_4^{2-}, NH_4^+, Na^+, K^+, Mg^{2+}, and Ca^{2+}). An online and continuous particulate carbon monitor (Model-4/OCEC (RT-4) Lab, Sunset Laboratory, Inc., USA) was used to measure the hourly OC and EC in $PM_{2.5}$. This OC/EC monitor adopts the thermal/optical method approved by National Institute for Occupational Safety and Health to measure the OC and EC collected on a quartz filter membrane.

The hourly mass concentrations of 25 elements (Ca, Al, Si, Fe, Ti, K, Zn, Mn, Pb, As, Ba, V, Cu, Cd, Ni, Cr, Ag, Se, Sb, Sn, Au, Ga, Tl, Pd and Co) were measured using an atmospheric heavy metal online monitor (XHAM-2000A, Hebei Sailhero Environmental Protection High-tech Co., Ltd., China). The hourly meteorological parameters were collected by applying meteorological sensors (FWS500, Fronttech, Ltd., China), including temperature (T), relative humidity (RH), air pressure (P), wind direction (WD), and wind speed (WS). The hourly solar radiations were measured using a pyranometer (CMP22, Kipp & Zonen B.V., Holland). The detailed parameters of the instruments are provided in Table S1.

To assess whether these measured chemical compositions were representative of the measured $PM_{2.5}$ mass concentration, the sum of WSIIs (Cl^-, NO_3^-, SO_4^{2-}, NH_4^+, Na^+, K^+, Mg^{2+}, Ca^{2+}), organic matter (OM), EC, and fine soils (FS) were used to reconstruct the mass concentration of $PM_{2.5}$, where OM and FS were calculated as follows (Malm et al., 1994):

$$OM = 1.6 \times OC \tag{1}$$

$$FS = 2.20 \times Al + 2.49 \times Si + 1.63 \times Ca + 2.42 \times Fe + 1.94 \times Ti \tag{2}$$

The reconstructed $PM_{2.5}$ exhibited strong correlations with the measured values ($R^2 = 0.80$), while explaining 73.0% of the measured $PM_{2.5}$ (Fig. S1), which means that these chemical species are representative of the measured $PM_{2.5}$. OM and mineral dust might be the main unexplained percentage of composition of the $PM_{2.5}$ (Watson et al., 2012; Chow et al., 2015).

2.3. Brief introduction of the PMF model

The US Environmental Protection Agency (EPA) PMF 5.0 model was used in this study to examine $PM_{2.5}$ source apportionment. Based on the observations made at the sampling site, PMF can decompose a matrix of the sample data (X) into two matrices: source profile (F) and source contribution (G) (Paatero and Tapper, 1994):

$$x_{ij} = \sum_{k=1}^{p} g_{ik} f_{kj} + e_{ij} \tag{3}$$

where x_{ij} is the jth species concentration measured in the ith sample, g_{ik} is the contribution of the kth source to the ith sample (factor time series), f_{kj} is the concentration of the jth species in the kth source (factor profiles), and e_{ij} is the residual matrix that cannot be explained by the model. To obtain the optimal factor resolution result, PMF defines the objective function Q, and finally resolves the g_{ik} and f_{kj} matrices that minimize the value of the objective function Q.

$$Q = \sum_{i=1}^{n} \sum_{j=i}^{m} \left(\frac{e_{ij}}{\sigma_{ij}} \right)^2 \tag{4}$$

where σ_{ij} is the measurement uncertainty. Two files are needed as input to run the PMF model, which are concentration and uncertainty (Unc) files, respectively. The uncertainty file calculation can be divided into two cases, when the concentration data was below the method detection limits of the instruments (MDLs, Table S1). The uncertainty is calculated using the following equation:

$$Unc = \frac{5}{6} \times MDL \tag{5}$$

When the concentration value was greater than the MDLs, the calculation of the Unc is calculated based on the following equation:

$$\text{Unc} = \sqrt{(\text{error fraction} \times \text{concentration})^2 + (0.5 \times \text{MDL})^2} \quad (6)$$

The missing values were replaced by the median concentration of a given species, with an uncertainty of four times the median, which is a recommended method in PMF analyses (Norris et al., 2014; Brown et al., 2015). In this study, the data were divided into four seasons: winter (1697 samples), spring (2208 samples), summer (2201 samples), and autumn (2184 samples). To consider the errors that are not considered as measurement, the extra modeling uncertainties of 6.0%, 10.0%, 9.0%, and 6.0% were used for winter, spring, summer, and autumn, respectively. The measured $PM_{2.5}$ was included as a total variable (weak species) and all other species were classified into three categories based on signal-to-noise ratio: "strong" species with a signal-to-noise ratio ≥ 1, "weak" species with 0.5 ≤ signal-to-noise ratio ≤ 1, bad species with a signal-to-noise ratio ≤ 0.5. Among all the input species, Ni and V had the S/N ratios of less than 0.5 in all the seasons and were labeled as bad, considering that Se and Cr had the S/N ratios less of than 0.5 in some seasons and less than 2.0 in all other seasons, they were labeled as bad. Cd, Sb, Sn and Ag all exhibited significant instability in the time series and were also labeled as bad considering that many values were below MDLs. For Ca^{2+}, Mg^{2+} K^+ and Na^+, many values were also found to be below the MDLs and were marked as bad. Considering that the signal-to-noise ratios of As in spring and summer were below 2 and the missing value was more than 50.0% of the total data, As was labeled as bad. As the data for the Al element exhibited large values at 3:00 am every night, Al was also labeled as bad. After the base run, it was found that R^2 between the fitted and measured values of Cu in spring was 0.40, and R^2 of Zn for autumn was 0.41, thus, these two species were labeled as weak, R^2 between the fitted and measured values of Cu in summer was 0.18, thus, it was labeled as bad. Considering the terms of EF diagnostics analysis, the nonrotated solution (F_{peak} = 0) was selected in the PMF model analysis. After 20 times base run based on the different values of seed, relatively consistent Q values were derived for all four seasons, with the winter, spring, summer, and autumn Q(true) and Q(Robust) values being 15,825.1 and 15,686.1, 19,353.5 and 19,314.8, 17,429.6 and 17,345.6, and 18,057.9 and 17,939.0, respectively. The results showed that the correlation between the model predicted and measured $PM_{2.5}$ for winter, spring, summer, and autumn were 0.84, 0.62, 0.70 and 0.81, respectively. To further evaluate the rotational ambiguity and measurement uncertainties in the derived PMF solutions, the bootstrap analysis and the displacement method were applied in this study. The results obtained fulfilled the criteria mentioned in the user guide and the discussion is provided in Supplementary Materials (Fig. S2).

3. Characteristics of particulate pollution

The annual average $PM_{2.5}$ concentration was 43.8 ± 27.6 μg·m^{-3} during the study period. Secondary inorganic aerosols (SIAs, i.e., the sum of sulfate, nitrate, and ammonium), OM, and FS were the major chemical species of $PM_{2.5}$ found during the study period, which accounted for 32.3%, 28.8%, and 23.5%, respectively (Fig. 2). Winter was found to be the most polluted season in Lanzhou, with an average $PM_{2.5}$ concentration of 72.8 μg·m^{-3}. Summer was the cleanest season with an average $PM_{2.5}$ concentration of 24.3 μg·m^{-3}, which was lower than the Chinese National Ambient Air Quality Standard (NAAQS) of $PM_{2.5}$ (35 μg·m^{-3}) (CAAQS, GB 3095-2012, https://www.transportpolicy.net/standard/china-air-quality-standards/). The average $PM_{2.5}$ concentrations during spring (39.2 μg·m^{-3}) and autumn (43.6 μg·m^{-3}) were slightly higher than this limit. Detailed concentrations of other species of $PM_{2.5}$ are provided in Supplementary Materials (Table S2). The contribution of SIAs to $PM_{2.5}$ concentration in winter (41.0%) was the largest among four seasons. The contribution of OM was relatively larger in winter (37.0%) and autumn (29.8%) than in spring (22.0%) and summer (26.6%). The contributions of FS were as high as 33.4% and 31.4% during spring and summer, respectively, with the contribution of SIAs being the lowest during spring (23.6%). Fine soils could not be ignored in this study as they accounted for more than 20.0% of $PM_{2.5}$ during spring, summer, and autumn. Generally, PM pollution during autumn and winter were characterized by the high fractions of SIAs and OM, while FS were evident during spring and summer.

The proportions of FS and SIAs have decreased and increased, respectively, in recent years when compared with a previous filter sampling based study conducted in Lanzhou in 2014 (Wang et al., 2016b), which revealed that annual average SIAs and FS accounted for 21.9% and 30.6% of $PM_{2.5}$, respectively. No significant change was found in the proportion of OM in recent years. The proportion of OM was higher while that of SIAs was significantly lower in Lanzhou than in Beijing and Tianjin (Xu et al., 2019). The seasonal variation in OM in Nanjing showed the opposite trend to Lanzhou, with the largest proportion of

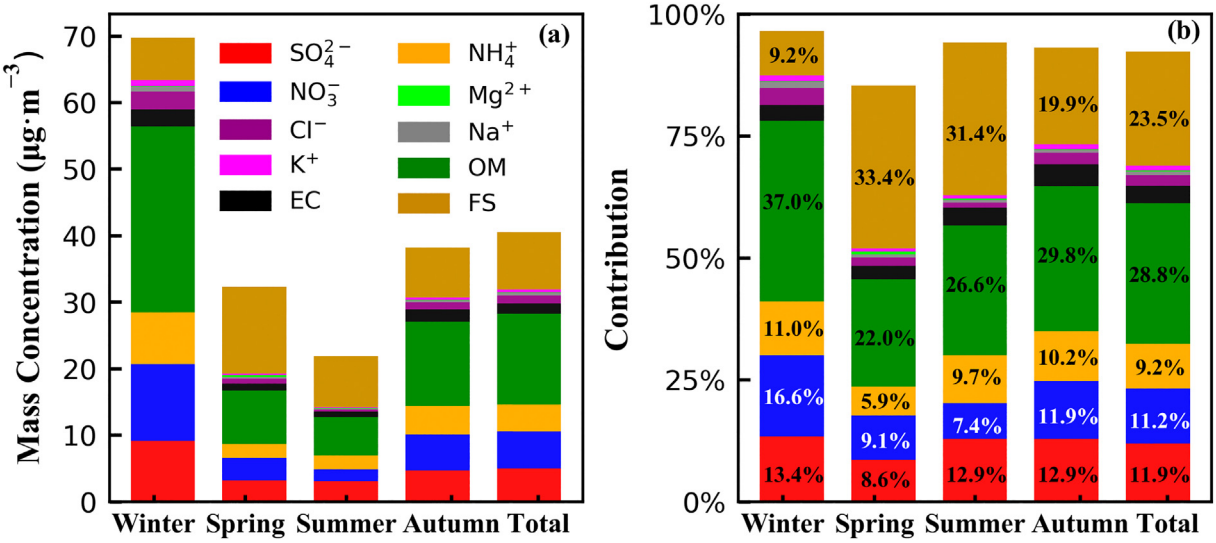

Fig. 2. Characteristics of particulate pollution at LACMS during the study period: (a) mass concentration and (b) contribution of aerosol species.

OM observed in summer and a smaller proportion in winter and spring (Li et al., 2016).

To better understand the formation mechanisms of heavy PM pollution in Lanzhou, the contribution of aerosol species from low to high PM pollution was investigated (Fig. 3). The contribution of SIAs was found to decrease with increasing $PM_{2.5}$ during winter, while OM remained relatively stable at ~40.0%. Both SIAs and OM contributions significantly decreased from low to high PM pollution, with their summation declining from ~60.0% to ~30.0% in spring. The contributions of FS remained high during spring and summer and decreased in autumn with increasing $PM_{2.5}$. Wintertime PM characteristics and formation mechanisms have been investigated in a previous study (Du et al., 2020), which suggested that vehicle emissions might be an important source of PM pollution in Lanzhou.

4. Contribution of different sources to PM pollution

4.1. PMF source appointment

The winter samples yielded 7 PM sources, vehicle emissions, secondary formation, coal combustion, smelting industry, mineral dust, power plant and fireworks (Fig. 4). Secondary formation referred to the formation of secondary inorganic aerosols. The source of vehicle emissions was characterized by the high fractions of OC and EC. A small amount of Cu has been found to emit from brake and tire wear of the vehicles (Karnae and John, 2011), and a small amount of ammonium has been found to emit from vehicles equipped with three-way catalytic converters (Chang et al., 2016). A significantly good correlation was found between this source and EC ($R = 0.91$). The extremely high fractions of SIAs and Cl^- defined the sources of secondary formation and coal combustion, respectively. Smelting industry source was characterized by the high fractions of Fe, Mn, and Zn (Mooibroek et al., 2011). A significantly good correlation was found between Mn and the source of smelting industry ($R = 0.95$). Power plant source was characterized by the high fractions of Pb, As, Zn and Cu in winter, when there was a heating period in Lanzhou. A wintertime power plant source was also found in a previous study conducted in Lanzhou (Tan et al., 2017). The high fractions of Earth's crustal elements (e.g., Fe, Ca, Si, and Ti) were found in the mineral dust source, which also exhibited good correlation with the constructed FS ($R = 0.78$). Good correlations among Fe and Ca, and Si further suggested the same source for these elements (Fig. S3). However, crustal elements Fe, Ca, and Si correlated poorly with Ba (Fig. S3), indicating a different emission source for Ba. This source only yielded during the traditional Spring Festival of China celebrated from 24 to 31 January 2020, characterized by the high fractions of Ba, Cu, and K (Ji et al., 2018). Relatively good correlations were also found among these three elements (Fig. S3), indicating that they originated from the same source.

The sources of coal combustion, vehicle emissions, and mineral dust were found to be relatively high in December 2019 and low in January

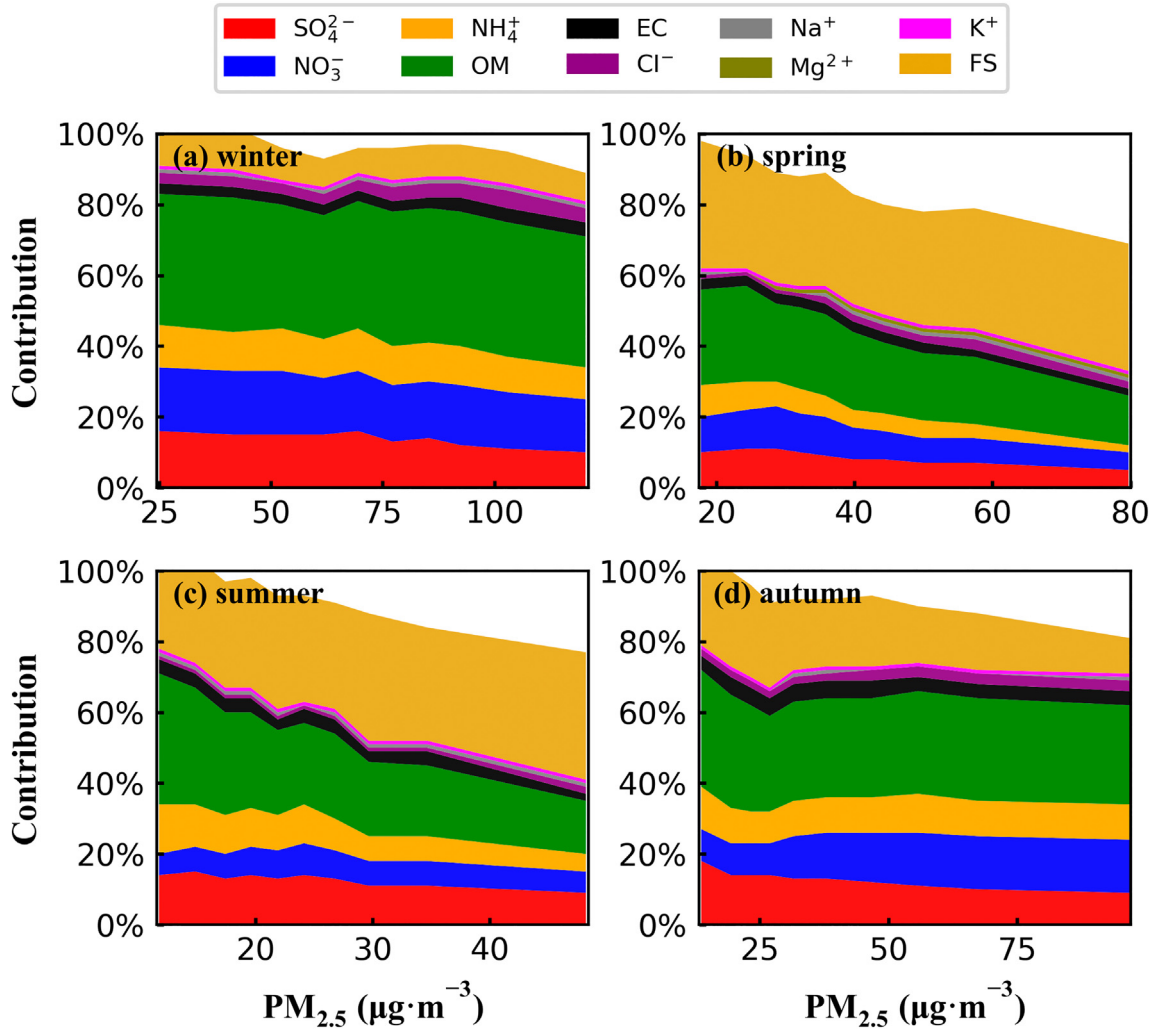

Fig. 3. Contribution of aerosol species from low to high PM pollution: (a) winter; (b) spring; (c) summer; and (d) autumn.

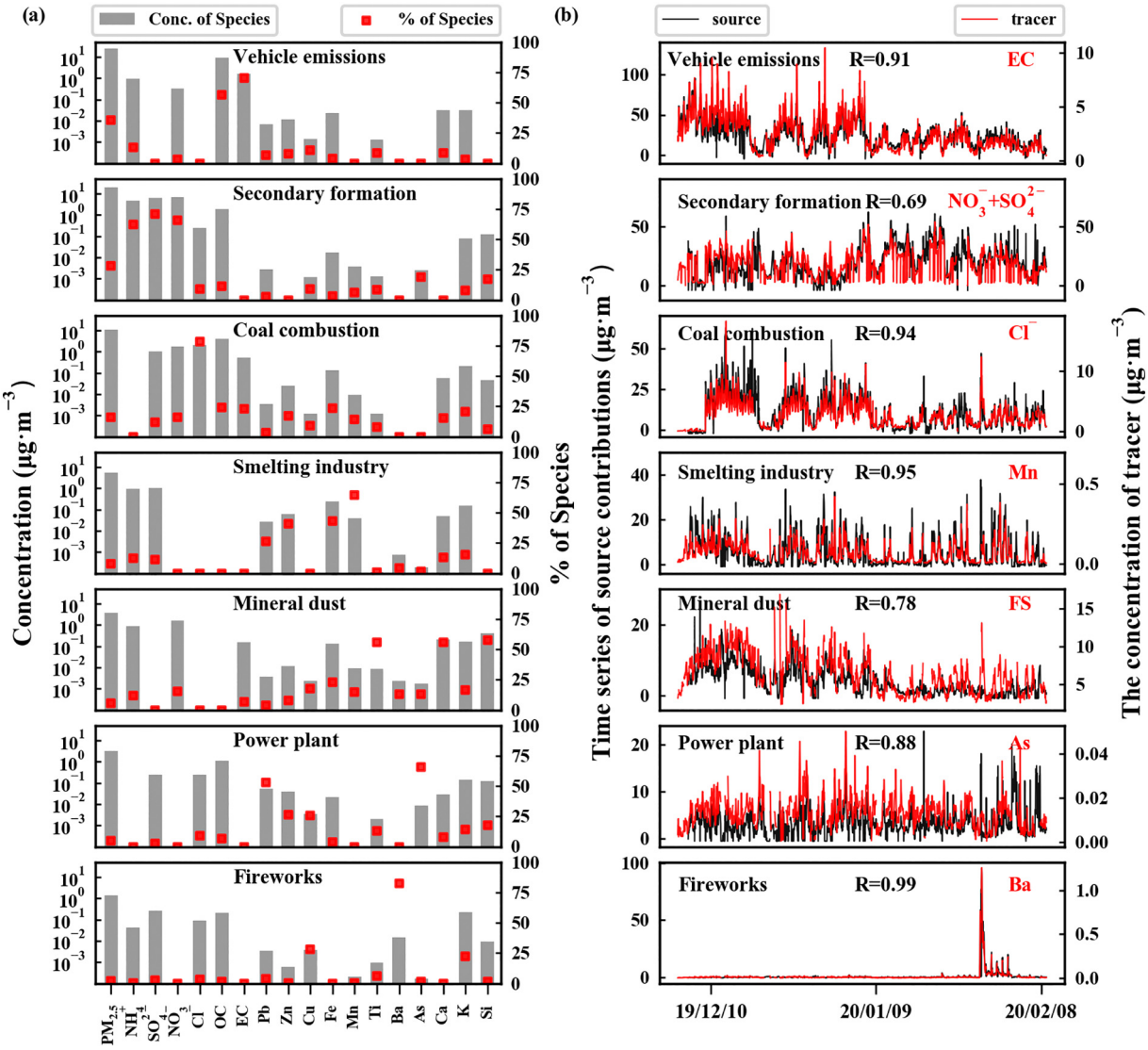

Fig. 4. The source profiles (bars) for the identified seven factors for $PM_{2.5}$ and the contribution percentages (red dots) in the PMF model (a) and the time series of sources (black line) and typical species (red line) (b) during winter in Lanzhou.

2020. Similar time series in the sources of mineral dust and vehicle emissions indicated that vehicles emitting road dust was an important contributor of wintertime mineral dust source. The sources of smelting industry and power plant exhibited large fluctuations accompanied by diurnal variations.

The spring samples yielded 5 PM sources, mineral dust, vehicle emissions, secondary formation, coal combustion, and mixed industrial emissions (Fig. 5). The springtime mineral dust source was also characterized by the high fractions of Earth's crustal elements (e.g., Fe, Ca, Si, Ti, and Ba). These elements exhibited higher correlation coefficients in spring than in the other seasons (Fig. S3). A significantly good correlation was found between the source of mineral dust and FS ($R = 0.97$), which was consistent with the frequently occurring dust events (floating dust, blowing dust, and dust storms) observed in spring in Northwest China (Tian et al., 2015). Furthermore, large differences were observed between the time series of mineral dust and vehicle emission sources, indicating that vehicles emitted road dust was not the main source of mineral dust during spring. Like winter, the springtime vehicle emission source was characterized by the high fractions of OC and EC, and good correlation was found between this source and EC ($R = 0.88$). A significantly good correlation was found between the source of secondary formation and the sum of nitrate and sulfate ($R = 0.91$). A mixed industrial emission source characterized by the high fractions of heavy metal elements (i.e., Zn, Pb, As and Mn) was identified in spring. The springtime sources of mixed industrial emission and coal combustion exhibited large fluctuations accompanied by the evident diurnal variations.

Summer was found to be the cleanest season, yielding six sources, i.e., vehicle emissions, mineral dust, secondary sulfate, secondary nitrate, coal combustion, and mixed industrial emission (Fig. 6). Most of the sources exhibited large fluctuations accompanied by the evident diurnal variations. Significantly good correlations were found for the sources and their tracers, indicating that these sources were independent in summer ($R \geq 0.88$). Thus, the secondary formation was further divided into secondary sulfate and secondary nitrate sources.

The autumn samples yielded seven sources, i.e., vehicle emissions, secondary nitrate, secondary sulfate, power plant, mineral dust, coal combustion, and smelting industry (Fig. 7). Significantly good correlations were found between the sources and their respective tracers ($R \geq 0.90$). A heavy pollution event was observed in early November which was evident in all sources and their respective tracers ($R \geq 0.90$). The PM pollution might also be enhanced by the gradually

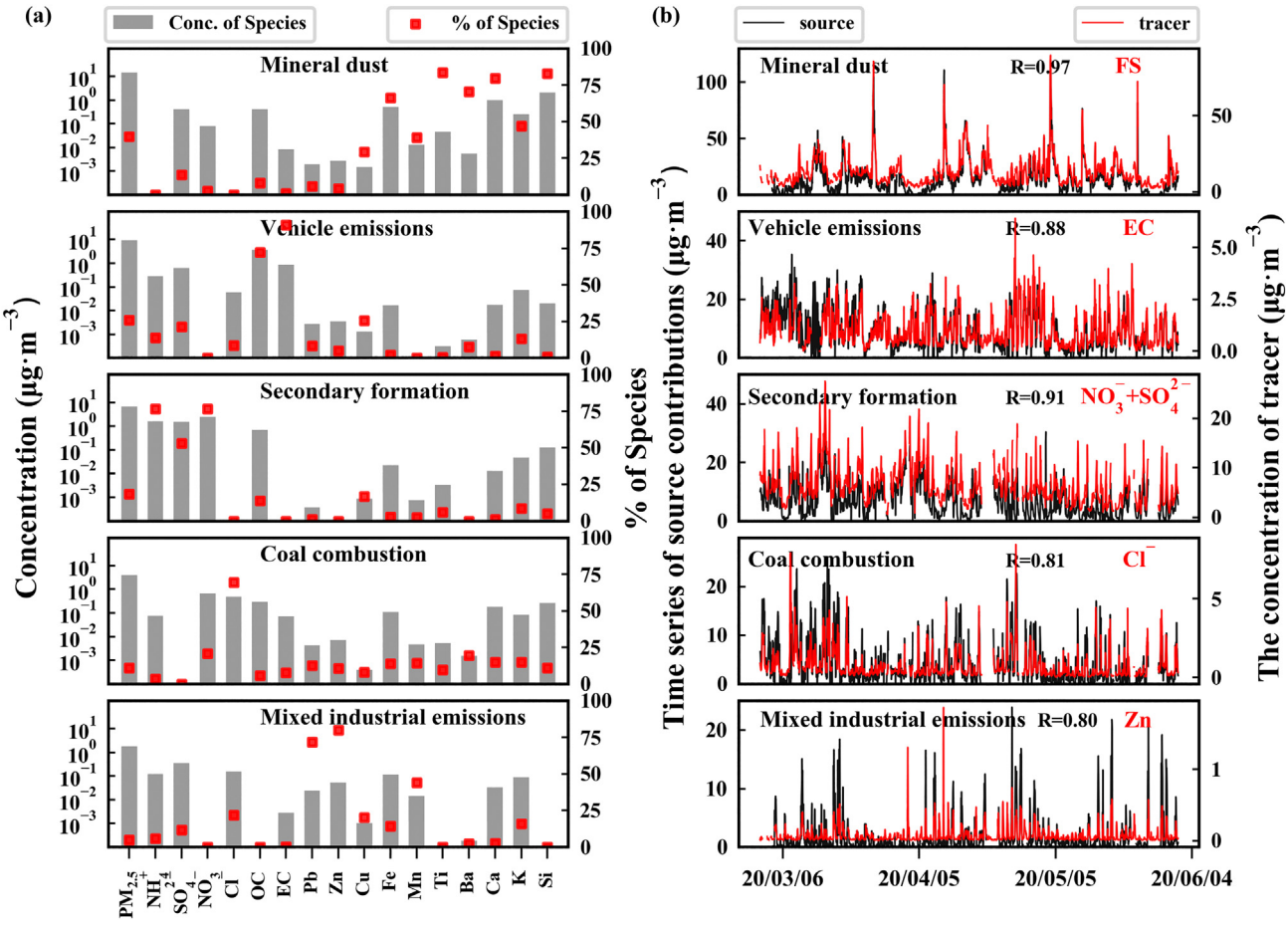

Fig. 5. The source profiles (bars) for the identified five factors for $PM_{2.5}$ and the contribution percentages (red dots) in the PMF model (a). The time series of sources (black line) and typical species (red line) (b) during spring in Lanzhou.

decreasing boundary layer height and the beginning of heating period in November.

To better understand the characteristics of PM sources in Lanzhou, contributions of PM sources in four seasons were further compared (Fig. 8). Vehicle emissions source was the largest contributor to PM pollution in autumn (56.6%) and winter (35.7%), followed by secondary formation that contributed 19.9% and 28.3% to fine PM pollution in autumn and winter, respectively. Coal combustion was also an important source observed in winter, contributing to 15.9% of the total PM pollution. In spring, the most important PM source was mineral dust (40.0%), which mainly originated from frequently occurring dust events (floating dust, blowing dust, and dust storms). Vehicle emissions (25.8%), secondary formation (18.4%), and coal combustion (10.9%) ranked second, third, and fourth important PM sources in spring, respectively. A comparable contribution was found for vehicle emissions (30.0%), mineral dust (30.0%), and secondary formation (28.9%) in summer.

Vehicle emissions were a major source in Lanzhou, accounting for the largest fraction of PM pollution in all seasons, except spring, when vehicle emissions ranked second to mineral dust emitted from natural sources. Specifically, vehicle emissions accounted for 56.6%, 35.7%, 30.0%, and 25.8% in autumn, winter, summer, and spring, respectively. Secondary formation was also an important source in Lanzhou, accounting for 28.9%, 28.3%, 19.9%, and 18.4% in summer, winter, autumn, and spring, respectively. Mineral dust was identified in all seasons, accounting for as high as 40.0% and 30.0% in spring and summer, respectively. Coal combustion accounted for 15.9%, 10.9%, 6.5%, and 5.6% in winter, spring, autumn, and summer, respectively. A relatively low contribution of mixed industrial emissions source was yielded in spring (5.0%) and summer (5.3%%). Power plant and smelting industry were identified in winter (4.6% and 7.8%) and autumn (6.7% and 2.0%). Fireworks was only yielded in winter because of the traditional Spring Festival of China.

Considering the relatively high PM pollution in winter and autumn in Lanzhou, vehicle emissions, secondary formation, and coal combustion, were found to be the most important anthropogenic PM sources in Lanzhou. In addition to vehicle emissions being identified through PMF, vehicles may create road dust and secondary formation may also be produced by vehicle exhaust (Almeida et al., 2020), which was also confirmed by the consistency in the time series of vehicle emissions and mineral dust sources in winter. Thus, the contribution of vehicles to PM pollution might be significantly higher than that obtained through the PMF results in this study. Mineral dust was also found to be an important PM source in Lanzhou originating from natural dust events and anthropogenic activities (e.g., road dust).

PMF source appointment has been previously conducted in Lanzhou based on a total of 60 offline filter samples collected in December 2012 and June to July 2013 (Tan et al., 2017). Tan et al. (2017) revealed that secondary formation accounted for the highest fraction of 33.0% of $PM_{2.5}$, followed by coal combustion (28.7%), mineral dust (13.3%), vehicle emissions (8.8%), steel industry (7.1%), smelting industry (6.0%), and power plant (3.1%) in winter. They further suggested that smelting industry (35.2%) was the highest contributor of PM pollution, with vehicle emissions being the second (25.2%) in summer. PMF source appointment has also been carried out using the samples collected in 2014 from a suburban petrochemical industrial site and a downtown site in Lanzhou (Wang et al., 2016b), which revealed that coal combustion (22.3%), mineral dust (21.8%), traffic emission (21.7%), and secondary formation (16.6%) were the most important PM sources. $PM_{2.5}$

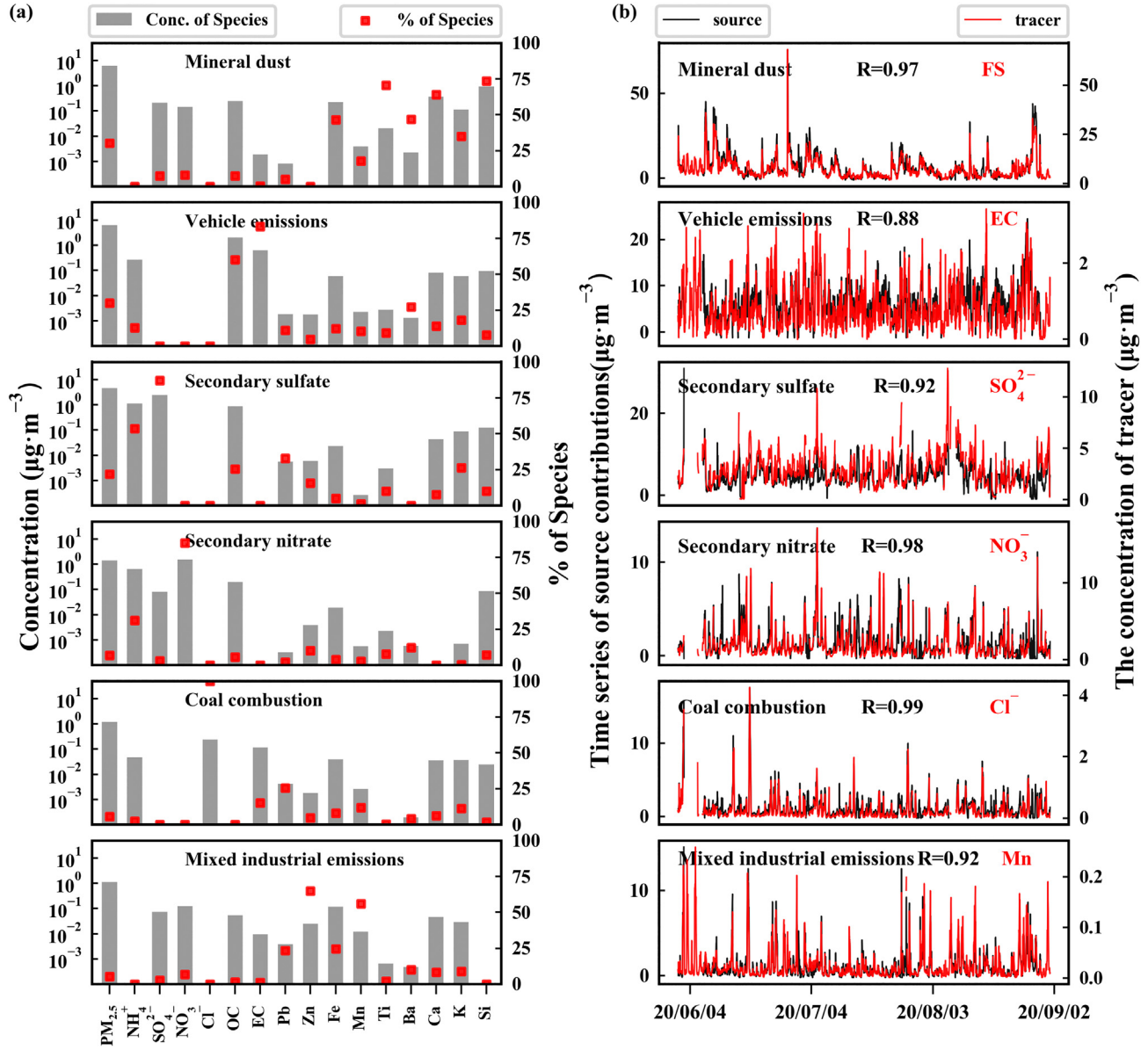

Fig. 6. The source profiles (bars) for the identified six factors for PM2.5 and the contribution percentages (red dots) in the PMF model (a). The time series of sources (black line) and typical species (red line) (b) during summer in Lanzhou.

concentrations in downtown Lanzhou were 120.5, 34.1, and 88.9 ± 52.0 μg·m^{-3} in December 2012, summer 2013, and 2014, respectively (Wang et al., 2016b; Tan et al., 2017), which were significantly higher than the $PM_{2.5}$ concentrations observed in this study.

Air pollution control in Lanzhou has achieved great success in recent years, during which the industrial emissions have gradually declined but vehicle numbers have rapidly increased (Chen et al., 2019; Du et al., 2020). Thus, vehicle emissions have become a major PM source. The contribution of vehicle emissions to PM pollution in some developed countries has already reached significantly high levels, for instance, 46.0% in the urban background site of Kozani city in Greece (Toils et al., 2014), 44.0% and 60.0% in the urban background and traffic sites of Ljubljana city in Slovenia, respectively (Saraga et al., 2021), and above 60.0% in central Los Angeles in USA (Sowlat et al., 2016).

4.2. Change in sources from low to high PM pollution

The contributions of the identified PM sources from low to high PM pollution were further studied (Fig. 9) to better understand the formation mechanisms of PM pollution in Lanzhou. The contribution of secondary formation decreased with increasing $PM_{2.5}$ in winter, spring, and summer, and that of vehicle emissions decreased with increasing $PM_{2.5}$ in spring and summer but increased in winter and autumn when PM pollution was relatively high. The contribution of vehicle emissions increased to ~40.0% and ~60.0% in winter and autumn, respectively, under heavy pollution conditions. The contribution of coal combustion gradually increased with increasing $PM_{2.5}$ in winter, and that of mineral dust rapidly increased to ~50.0% and 40.0% in spring and summer, respectively.

The contribution of secondary sulfate and biomass burning decreased while that of secondary nitrate and secondary organic aerosol increased with increasing $PM_{2.5}$ in Shenzhen, China (Su et al., 2020). In the Beijing-Tianjin-Hebei region of China, the contribution of secondary sources increased while that of vehicle emissions decreased with increasing $PM_{2.5}$. The trend for vehicle emissions was contrary to the winter and autumn results in this present study. The contribution of vehicle emissions reached ~45.0% during the clean period ($PM_{2.5}$ < 75 μg·m^{-3}) in Beijing in winter (Huang et al., 2017). The high contribution of vehicle emissions in Lanzhou is further discussed in Section 5.3.

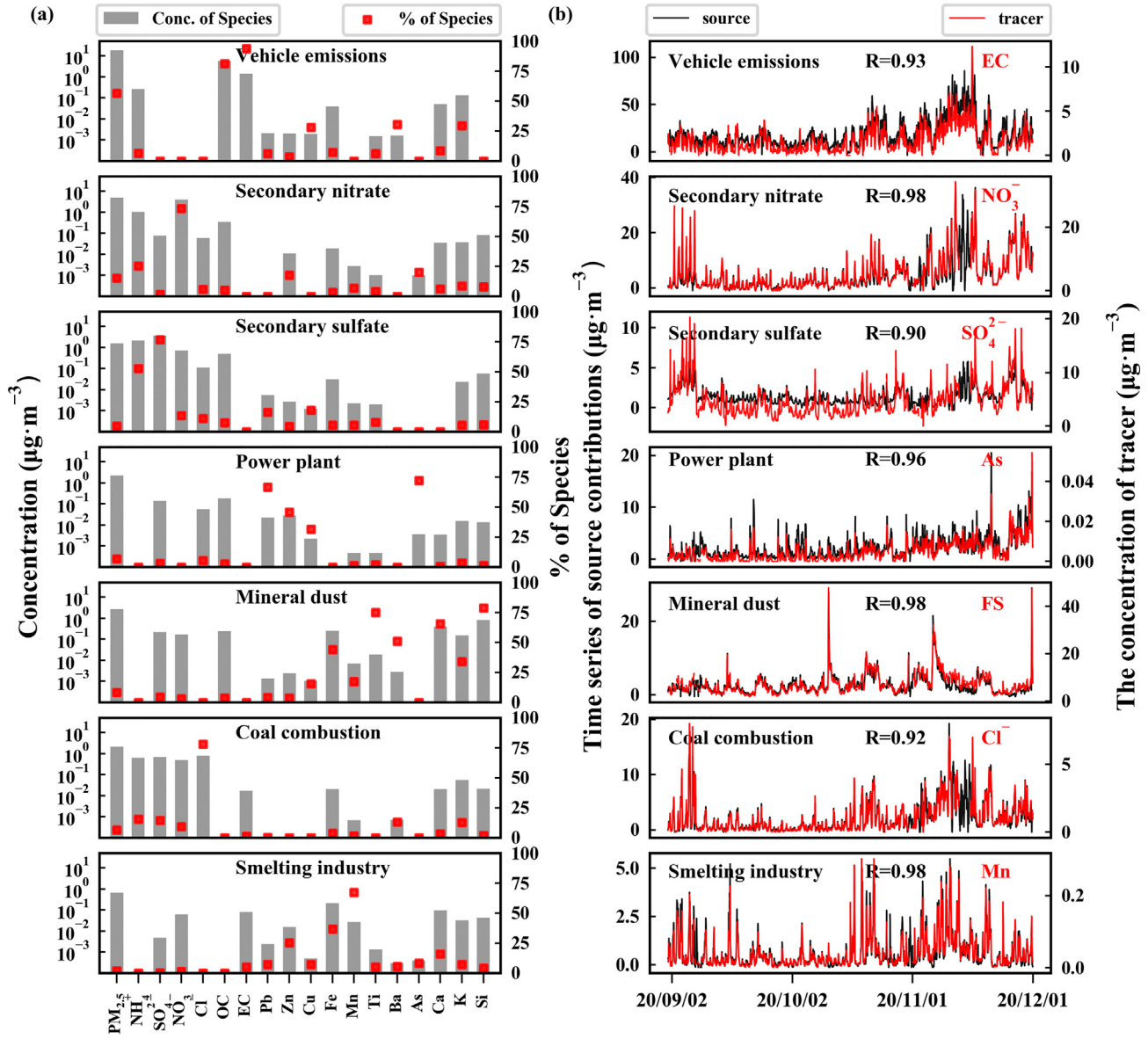

Fig. 7. The source profiles (bars) for the identified seven factors for $PM_{2.5}$ and the contribution percentages (red dots) in the PMF model (a). The time series of sources (black line) and typical species (red line) (b) during autumn in Lanzhou.

4.3. Contribution of vehicle emissions to EC

Vehicle emissions were the highest source of EC in downtown Lanzhou during the study period (Fig. 10), accounting for 70.3%, 91.0%, 83.5%, and 93.7% of the total EC in winter, spring, summer, and autumn, respectively. Coal combustion was the second important source of EC, accounting for 23.0%, 8.0%, 15.0% of the total EC in winter, spring, and summer, respectively. Smelting industry also contributed to 5.0% of the total EC in autumn. An interesting result was that mineral dust contributed 7.0% and 1.0% to the total EC in winter and spring, respectively, which might have originated from the EC present on the surface of soil dust (Schmidt and Noack, 2000; Gautam et al., 2020).

Studies have revealed that EC in the urban areas of China are mainly emitted from vehicle emissions. For example, EC from vehicle emissions account for 77.3% of the total EC in winter in Linfen from 2108 to 2019 (Li et al., 2020), 50.6% in winter in Shijiazhuang from 2017 to 2018 (Zhang et al., 2020), 54.0% in Shanghai in the winter of 2013 (Wei et al., 2019), 52.9% of the annual average and 65.2% of the total EC in spring in Beijing from 2017 to 2018 (Cui et al., 2021), and 60.0% of the total BC in Shenzhen in autumn 2019 (Su et al., 2020). The contribution of vehicle emissions to EC was found to be higher in some American and European cities, BC from vehicle emissions accounted for ~80.0% of the total BC in Patras, Greece (Manousakas et al., 2017), 87.0% of the total BC in Pittsburgh, USA (Lambe et al., 2009), and ~ 95% of the total EC in the West Midlands conurbation, United Kingdom (Yin et al., 2010). A high contribution reported in these developed countries was like the results obtained in this study, except for winter, which was affected by coal combustion. This implied that vehicle emissions were the main source of EC in the urban areas where industrial emissions were well controlled.

4.4. Diurnal variations of PM sources

For the first time, the hourly online data of the PM species made the investigation of diurnal variations of the PM sources possible in Lanzhou (Fig. 11). In this study, only the most important four sources, vehicle emissions, secondary formation, coal combustion, and mineral dust, were studied. Meteorological parameters include RH, WS, T, and solar

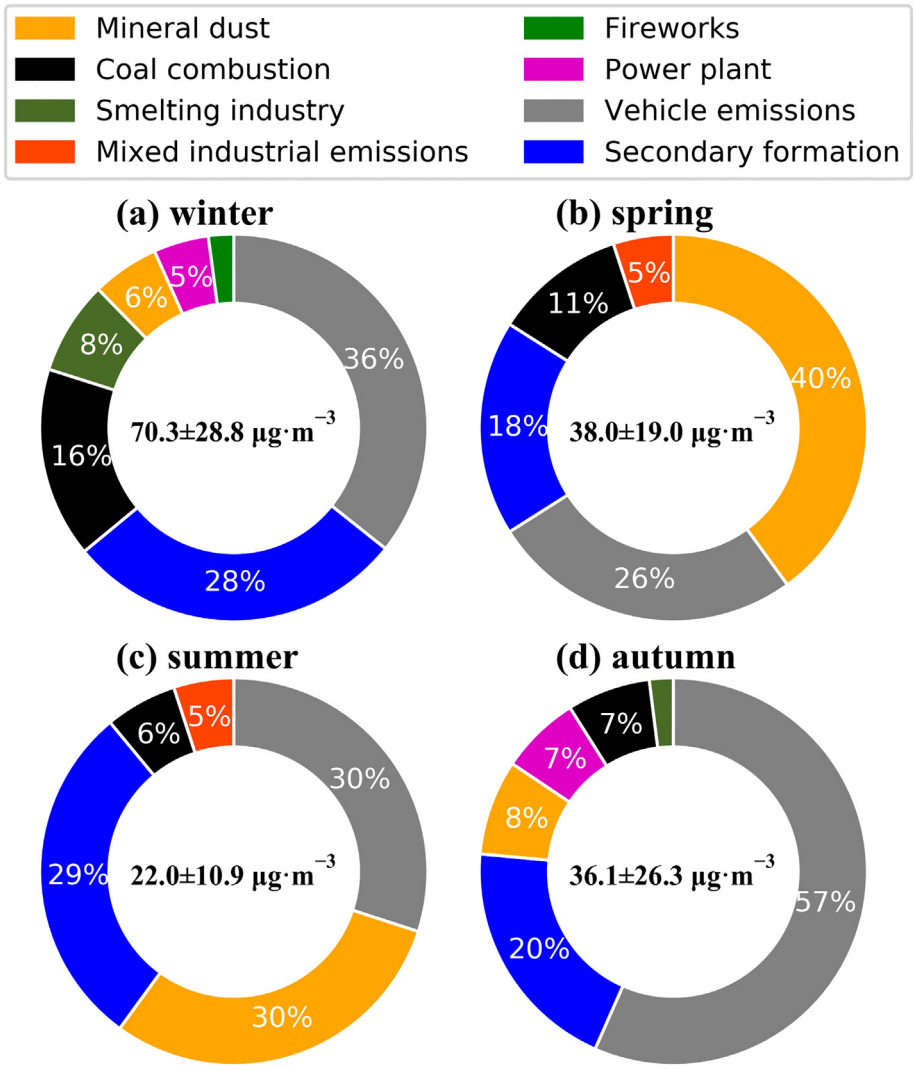

Fig. 8. Contributions of PM sources in (a) winter; (b) spring; (c) summer; and (d) autumn in Lanzhou. The sources of secondary sulfate and secondary nitrate were summed up to the source of secondary formation for better comparison.

radiation were analyzed to understand the diurnal variation of these PM sources. Anthropogenic sources exhibited obvious diurnal variations, while mineral dust that mainly originated from natural sources showed little diurnal variation.

Morning rush hours caused apparent peaks in vehicle emissions in the four seasons, but specific peak hours varied with seasons, which were 11:00, 10:00, 09:00, 08:00, in winter, autumn, spring, and summer, respectively. These peaks occurred earlier in warm seasons (spring and summer) and later in cold seasons (autumn and winter), which might be related to the waking up time of the residents. Daytime low concentrations in vehicle emissions in the four seasons were caused by the presence of favorable diffusion conditions such as high boundary layer height and wind speed (Zhang et al., 2021; Fig. 11f). Vehicle emissions increased as the evening rush hours began at 17:00, which was because of the combination of increasing vehicle numbers and worsening dispersion conditions. Then vehicle emissions in the cold seasons rapidly increased to higher than those of the morning rush hour peaks while those in the warm seasons gradually increased and never exceeded the values of the morning rush hour peaks. A peak was observed in vehicle emissions after the evening rush hours in winter (20:00), which was like those observed in other cities, such as Beijing (Cui et al., 2021). However, no obvious peaks were observed in the other three seasons. The increase in vehicle emissions after the evening rush hours was further enhanced by the movement of heavy-duty vehicles during nighttime. Vehicle emissions during the cold seasons were higher than those in the warm seasons, which was probably because of the unfavorable diffusion conditions present during the cold seasons and favorable ones present during the warm seasons. Vehicle emissions in the cold seasons decreased during the nights and increased at dawn, while those in the warm seasons remained relatively high from the midnight to next morning. The decrease in vehicle emissions during nighttime in the cold seasons was explained by the very low ambient temperatures during the nights in autumn and winter in Northwest China. Extremely low ambient temperatures during the nights in winter resulted in less vehicle movement than that in autumn, but more unfavorable diffusion conditions also contributed to higher accumulations in winter, resulting in comparable vehicle emissions from midnight to next morning in these two seasons. The reduction in vehicles from midnight to next morning in winter may be compensated by more vehicles from morning to midnight, thus, resulting in higher vehicle emissions than that in autumn.

Secondary formation in winter was significantly higher than those in the other seasons (Fig. 11b), mainly because of high PM pollution in winter. The diurnal variation of secondary formation was explained by the diurnal variation of the sulfur and nitrogen oxidation ratios (SOR and NOR) that were studied by Du et al. (2020). Low SORs in the

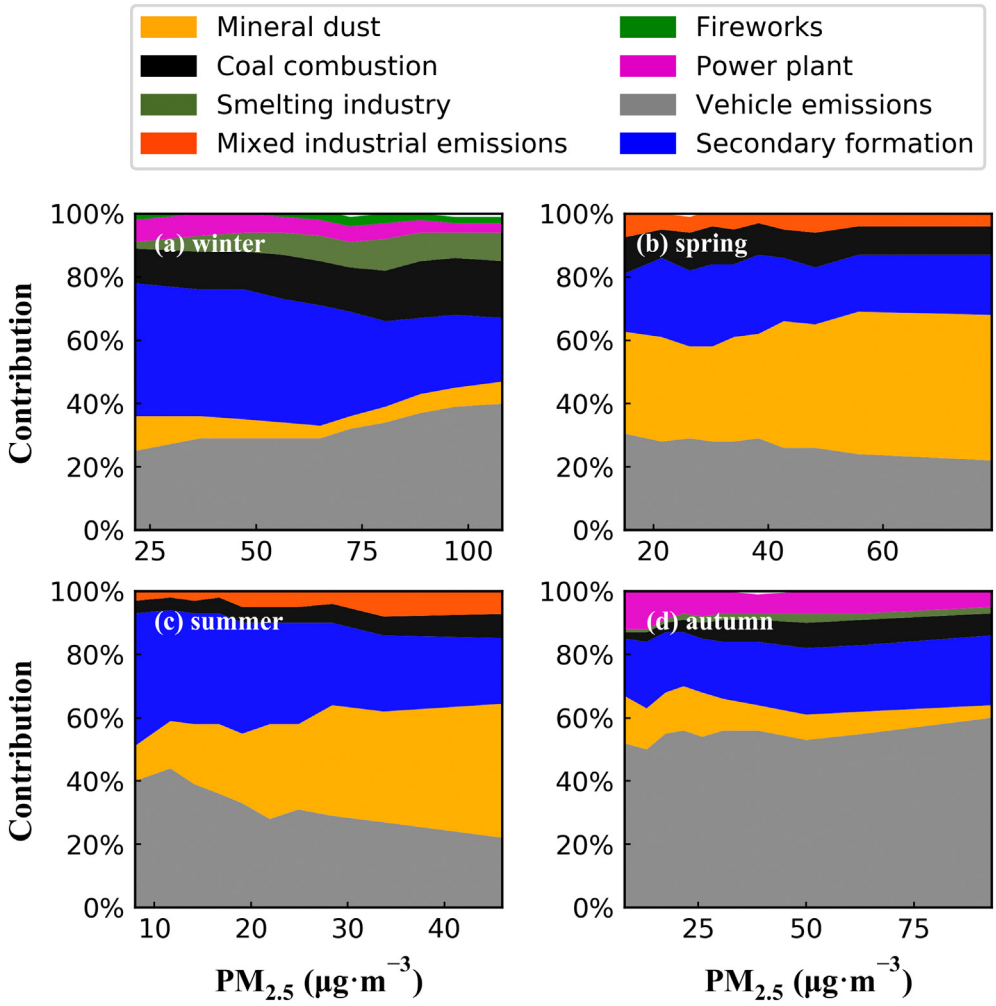

Fig. 9. The contribution of identified PM sources from low to high PM pollution: (a) winter; (b) spring; (c) summer; and (d) autumn. The sources of secondary sulfate and secondary nitrate in summer and autumn are added up to the source of secondary formation for better comparison.

morning led to low secondary formation in winter. Peak values were found in SOR from 17:00 to 19:00 and in NOR at 16:00, leading to peak values in secondary formation from 15:00 to 18:00 in winter. Secondary formations were comparable in spring and autumn when $PM_{2.5}$ concentrations were also comparable. Relative humidity and radiation were the most important factors that affected the secondary formation of aerosols from photochemistry and aqueous phase generations. Relative humidity in spring was lower than that in autumn but opposite was observed for radiation, which resulted in comparable secondary formation in these seasons. $PM_{2.5}$ in summer was significantly lower than those in the other seasons but secondary formation was close to those in spring and autumn, which was attributed to a high secondary formation efficiency due to strong radiation and high RH in summer. Thus, the contribution of secondary formation was the highest (28.9%) in summer. The increase in secondary formation from midnight to next morning in summer was explained by increasing aqueous phase chemistry facilitated by increasing humidity.

Wintertime coal combustion was significantly higher than those of the other seasons (Fig. 11c), resulting from the coal combustion from residential heating and unfavorable diffusion conditions during winter. Generally, coal combustion source exhibited an evident peak around noon (at 11:00, 10:00, 11:00, and 13:00 in spring, summer, autumn, and winter, respectively), which subsequently decreased until late evening, and then gradually increased from late evening to next morning, except in winter. Another peak comparable to the daytime one was found at midnight in winter, which was caused by coal combustion from residential heating at midnight when the temperature was significantly below zero.

Springtime dust events (floating dust, blown dust, and dust storms) originating from Taklimakan and Gobi deserts frequently occurred in Northwest China (Huang et al., 2010; Tian et al., 2015), leading to a very high mineral dust in spring (Fig. 11d). Mineral dust was found to mainly originate from natural dust events, and it exhibited little diurnal variation in the four seasons. However, it slightly increased after midnight in spring and summer and increased in the morning in winter when the ground soil was dry, which might be attributed to more heavy-duty vehicle movement in warm seasons at nighttime and in cold seasons at daytime.

5. Discussion

5.1. Transport of mineral dust

Lanzhou is a relatively isolated city where regional transport of PM and the precursors are less important to PM pollution. Thus, only the transport of mineral dust in spring and summer was studied. The Potential source contribution function (PSCF) results (Fig. S4) revealed that spring dust originated from three source regions: (1) Turpan Basin, Taklimakan desert, and northern Xinjiang located in the northwest of Lanzhou; (2) Gobi desert and Mongolia located in the north of Lanzhou; (3) Kerchin Sands in Inner Mongolia and Yamarek Desert located in the northeast of Lanzhou. Mineral dust in summer mainly originated in

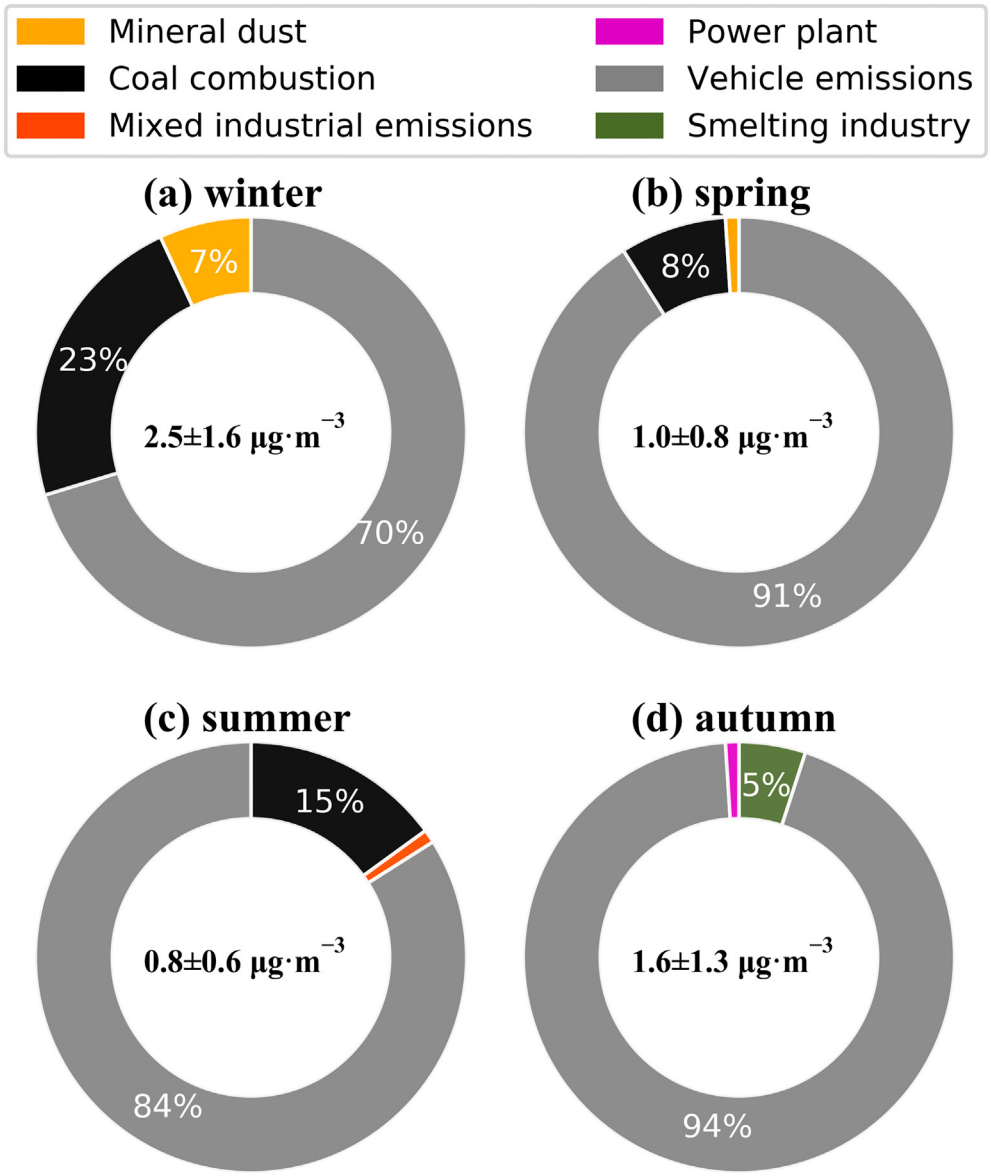

Fig. 10. Contribution of PM sources to EC: (a) winter; (b) spring; (c) summer; and (d) autumn.

from northwest of Lanzhou, i.e., Hexi Corridor and Xinjiang. Gobi Desert also contributed to a few dust events in summer.

5.2. Influence of meteorological factors on PM sources

The relationships between meteorological factors and PM sources were studied to better understand the local scale influence of meteorological conditions on PM pollution (Fig. 12). The high concentration of vehicle emissions was characterized by low wind speed in the cold seasons (winter and autumn), indicating the local origination of vehicle emissions accompanied by unfavorable diffusion conditions. Large values at low wind speed were less pronounced in spring and summer because of relatively low concentration of vehicle emissions.

As the winter secondary formation was the highest among the four seasons and the low values were significantly larger than the high values of the other three seasons, the winter secondary formation showed large values in all directions and wind speed, but the strong western winds continued to bring the relatively higher concentrations of pollutants. The higher concentrations of pollutants from strong western winds were also observed in spring and autumn, which was explained by the industrial emissions of Xigu district.

The high concentrations of mineral dust mainly originated from northeast in spring and west in summer, which were consistent with the PSCF results discussed in Section 5.1. The high concentration of coal combustion originated from west in the relatively strong coal combustion seasons (winter, spring, and autumn) because industries and power plants are in the Xigu district.

5.3. Reasons for the high contribution of vehicle emissions

The contribution of vehicle emissions was found to be 35.7% in winter when PM pollution was the highest, and as high as 56.6% in autumn based on the PMF analysis. Vehicle emissions were the largest estimated PM source for the total samples collected in this study, accounting for 37.0% of fine PM pollution during the study period from December 2019 to November 2020. The largest contribution of vehicle emissions to fine PM pollution was further validated by another source appointment model called Unmix (Henry, 2003), which yielded an annual vehicle emission contribution of 30.5% (Fig. S5 and Table S3). Considering the potential contribution of vehicle emissions on secondary formation and mineral dust (Almeida et al., 2020), its contribution might be significantly higher than the values estimated by the PMF model.

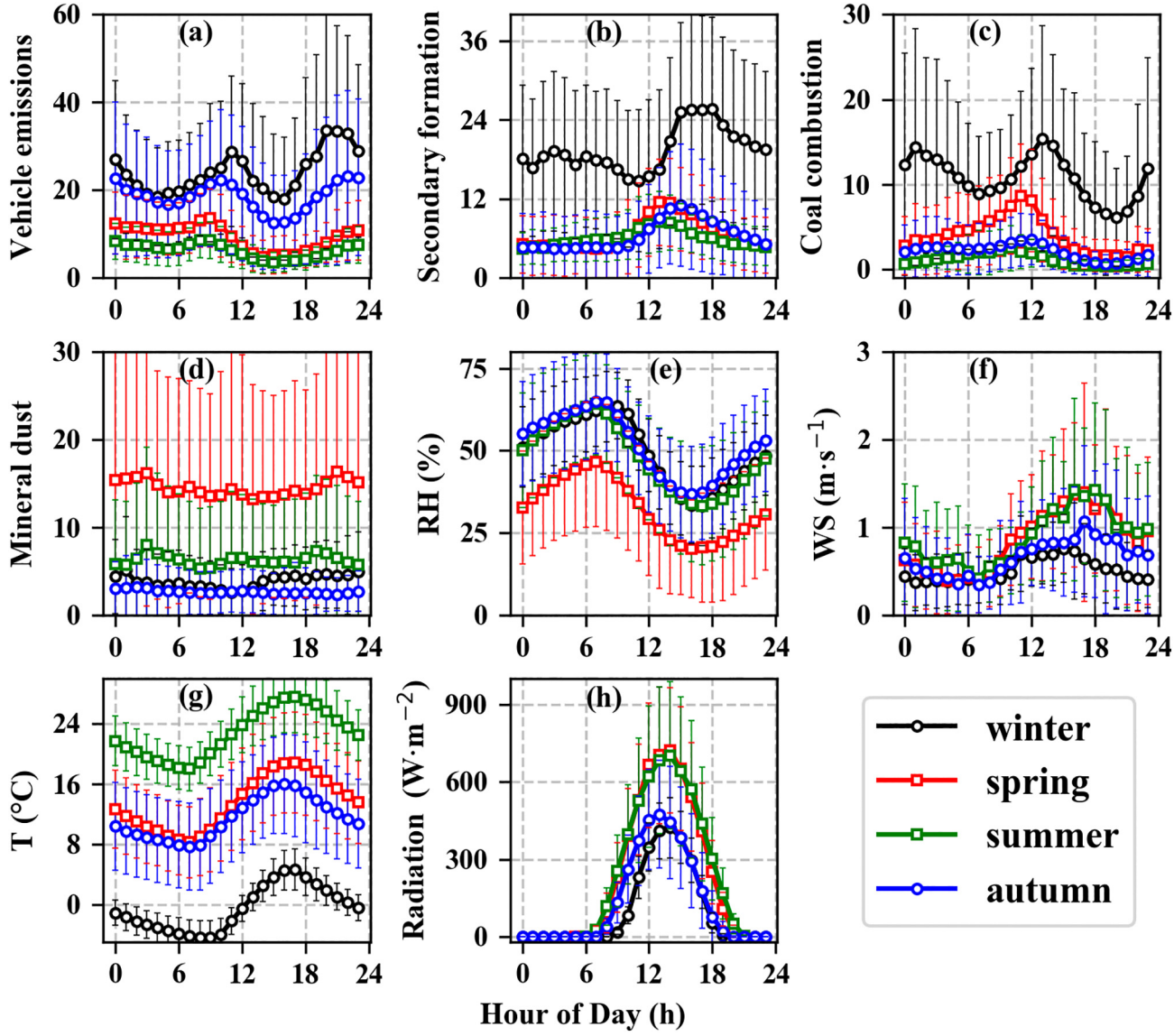

Fig. 11. Diurnal variation of the identified main PM sources and meteorological parameters (a) vehicle emissions; (b) secondary formation; (c) coal combustion; (d) mineral dust; (e) relative humidity; (f) wind speed; (g) temperature; and (h) radiation.

The relatively decreasing industrial emissions and increasing motor vehicle numbers were other reasons that led to a high contribution of vehicle emissions in Lanzhou and other cities of China. PMF analysis carried out for the Chinese cities revealed that the contribution of vehicle emissions generally increased from 1987 to 2017 (Zhu et al., 2018). For example, the contribution of vehicle emissions to $PM_{2.5}$ increased from ~10.0% in January 2013 to 38.7% in January 2018 in a typical mixed residential, cultural, and transportation zone in Beijing (Zhong et al., 2020). The increase in vehicle emissions in an urban site in Beijing was verified in more detail by Chen et al. (2019). For example, the contribution of vehicle emissions in urban Beijing increased from 19% in March 2013 to 29% in November 2016, subsequently to 40% in November 2017, and finally to 54% in March 2018 (Chen et al., 2019). A contribution of 23.0% was obtained using the hourly measurements taken from June 2016 to May 2017 in urban Beijing (Cui et al., 2021), 26.5% derived from the measurements taken from November 2018 to January 2019 in urban Linfen (Li et al., 2020), and 29.2% derived from the measurements taken from March 2017 to February 2018 in urban Wuhan (Huang et al., 2019). The contribution of vehicle emissions was as high as 31.7% in the USA EPA Chemical Speciation Network for over 200 sites from 2000 to 2005 (Thurston et al., 1994), and higher than 30.0% in some European cities in recent years, for instance, 33.0% in the city center of Patras, Greece (Manousakas et al., 2017), 35.0% at an urban background site in Bologna, Italy (Tositti et al., 2014), 31.3% in an urban background site in Warsaw, Poland (Juda-Rezler et al., 2020).

Unfavorable diffusion conditions and semi-arid climate were also responsible for the high contribution of vehicle emissions in Lanzhou. The Lanzhou basin is situated in a narrow valley of the Yellow River and the surrounding mountains are higher than the boundary layer height in winter, creating significantly bad diffusion conditions for air pollutants. Dry climate is unfavorable for converting gaseous pollutants to PM pollutants in the atmosphere, which leads to a higher contribution of primary emissions from the vehicles than secondary PM pollutants. During heavy PM pollution, the exchange of urban air pollutants and clean air in the surrounding areas was limited and secondary formation was also weakened, both of which led to a high contribution of vehicle emissions. The PMF analysis showed the high contributions of vehicle emissions in cities worldwide with unfavorable diffusion conditions. For example, the contributions of vehicle emissions have been found to be 46.0%, 44.5%, 44.0%, 40.9%, and 39.0% in an urban background

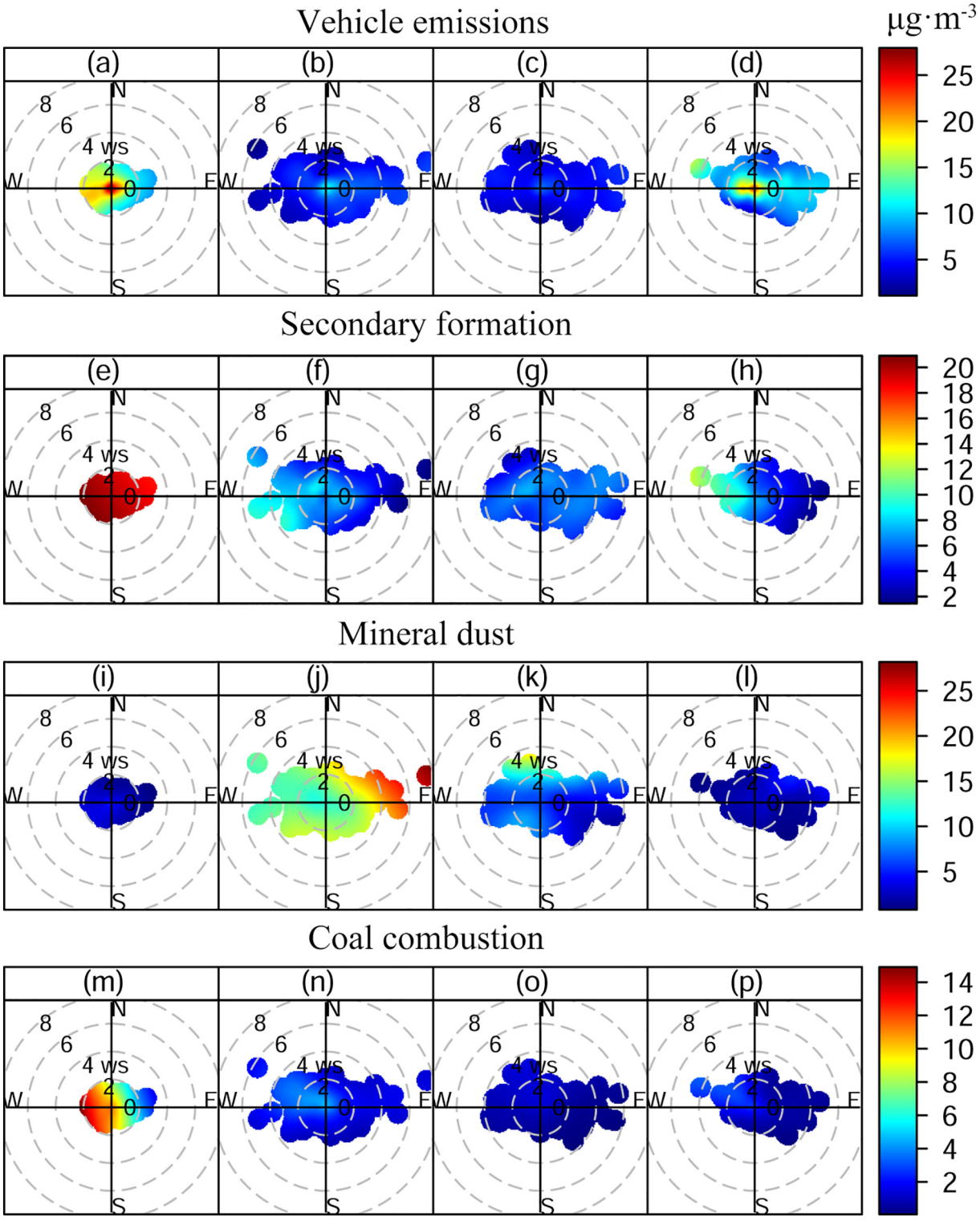

Fig. 12. The bivariate polar plots of sources in four seasons. The plots from top to bottom panels represent sources of vehicle emissions, vecondary formation, mineral dust, and coal combustion. The plots from left to right panels represent seasons of winter, spring, summer, and autumn.

site of Kozani, Greece (Toils et al., 2014), in sites in residential areas of Tehran, Iran (Esmaeilirad et al., 2020), in an urban background site of Ljubljana, Slovenia (Saraga et al., 2021), in a traffic site and an industrial site in Monterrey, Mexico (Martínez-Cinco et al., 2016), and in a site in central Santiago, Chile (Barraza et al., 2017), respectively. These cities experience unfavorable diffusion conditions, such as basin topography, river valley terrain, or surrounded by mountains to some extent. Unfavorable diffusion conditions resulting in the high contribution of vehicle emissions can be further validated by the seasonal variation in the contribution of vehicle emissions. For example, the contribution of vehicle emissions has been found to be higher during warm seasons than the cold seasons (Barraza et al., 2017). Dry climate was found for these cities

except Santiago. Semi-arid climate was found for Tehran and Monterrey. Dry climate is also favorable in emitting road dust into the atmosphere.

6. Summary and conclusions

Quantitative estimation of the contribution of the sources to PM pollution is essential but limited because of the contribution of the sources as well as the sources themselves exhibiting temporal and spatial variations. The high-resolution online data of $PM_{2.5}$, organic carbon (OC), elemental carbon (EC), water-soluble ions, and elements was used to conduct PM source appointment from December 2019 to November 2020, with an emphasis on the contribution of vehicle emissions to fine PM pollution in Lanzhou. Main findings are summarized below.

The average $PM_{2.5}$ concentration was found to be 43.8 ± 27.6 $\mu g \cdot m^{-3}$ during the study period. The SIAs, OM, and FS were found as the the major chemical species of $PM_{2.5}$ during the study period, accounting for 32.8%, 28.8%, and 23.5%, respectively. Winter was observed as the most polluted season in Lanzhou, with an average $PM_{2.5}$ concentration of 72.8 $\mu g \cdot m^{-3}$. The contribution of SIAs decreased with increasing $PM_{2.5}$ during winter, while OM contribution remained relatively stable at ~40.0%.

Vehicle emissions, secondary formation, mineral dust, and coal combustion were found as the major PM sources using the PMF model. Vehicle emissions accounted for 56.6%, 35.7%, 30.0%, and 25.8% in autumn, winter, summer, and spring, respectively. Secondary formation was also an important source in Lanzhou, accounting for 28.9%, 28.3%, 19.9%, and 18.4% in summer, winter, autumn, and spring, respectively. Mineral dust was identified in all the four seasons and accounted as high as 40.0% and 30.0% in spring and summer, respectively. Coal combustion accounted for 15.9%, 10.9%, 6.5%, and 5.6% in winter, spring, autumn, and summer, respectively. Other sources contributed less than 10.0% in all seasons. Considering the relatively high PM pollution in winter and autumn in Lanzhou, vehicle emissions, secondary formation, and coal combustion, were found to be the three most important anthropogenic PM sources in Lanzhou.

The contribution of secondary formation decreased with increasing $PM_{2.5}$ in winter, spring, and summer. The contribution of vehicle emissions decreased with increasing $PM_{2.5}$ in spring and summer but increased in winter and autumn when PM pollution was relatively high. The contribution of vehicle emission source increased to ~40.0% in winter and ~60.0% in autumn.

Vehicle emissions were the highest source of EC in downtown Lanzhou, accounting for 70.3%, 91.0%, 83.5%, and 93.7% of the total EC in winter, spring, summer, and autumn, respectively. Coal combustion was the second important source of EC, accounting for 23.0%, 8.0%, 15.0% of the total EC in winter, spring, summer, respectively. Mineral dust accounted for 7.0% and 1.0% of the total EC in winter and spring, respectively, which might have originated from the EC present on the surface of the soil dust.

Evident diurnal variations were observed in the anthropogenic sources of vehicle emissions, secondary formation, and coal combustion, while mineral dust that mainly originated from natural sources exhibited little diurnal variation. The peaks for vehicle emissions during the morning rush hours seemed to be appear earlier in warm seasons and later in cold seasons, which might be related to the waking up time of the residents. Both atmospheric diffusion conditions and human activities contributed to the diurnal variations in these anthropogenic sources.

The relatively decreasing industrial emissions and increasing motor vehicle numbers was one of the reasons that led to the high contribution of vehicle emissions in Lanzhou and other cities of China. Unfavorable diffusion conditions and semi-arid climate were also responsible for the high contribution of vehicle emissions in Lanzhou, which was also found in some other cities that were suffering from unfavorable diffusion conditions. With the reduction in industrial emissions and increase in vehicle numbers in China, vehicle emissions are going to be the largest source of urban PM pollution. To sustainably improve air quality in Chinese cities, efforts should be made to control vehicle emissions such as promoting clean-energy vehicles and encouraging public transportation.

CRediT authorship contribution statement

Min Wang: Methodology, Formal analysis, Data curation, Software, Writing – original draft, Writing – review & editing, Visualization. **Pengfei Tian:** Conceptualization, Formal analysis, Writing – original draft, Writing – review & editing, Project administration, Funding acquisition, Methodology, Validation, Investigation. **Ligong Wang:** Methodology, Writing – original draft, Visualization. **Zeren Yu:** Visualization. **Tao Du:** Visualization. **Qiang Chen:** Methodology, Formal analysis. **Xu Guan:** Formal analysis, Investigation. **Yumin Guo:** Visualization. **Min Zhang:** Visualization. **Chenguang Tang:** Methodology, Formal analysis. **Yi Chang:** Resources. **Jinsen Shi:** Data curation, Resources. **Jiening Liang:** Formal analysis. **Xianjie Cao:** Formal analysis. **Lei Zhang:** Funding acquisition, Supervision.

Declaration of competing interest

The authors declare that they have no known competing financial interests or personal relationships that could have appeared to influence the work reported in this paper.

Acknowledgments

This research was supported by the National Natural Science Foundation of China (41905017), the Foundation for Innovative Research Groups of the National Natural Science Foundation of China (41521004), and the Fundamental Research Funds for the Central Universities (lzujbky-2020-36). The authors thank the staffs from the Lanzhou Atmospheric Components Monitoring Superstation (LACMS) for the online particulate pollution data and supporting data. The data is available online at the Semi-Arid Climate and Environment Observatory of Lanzhou University (SACOL, http://climate.lzu.edu.cn/English/Data_Sharing/LACMS_data.htm).

Appendix A. Supplementary data

Supplementary data to this article can be found online at https://doi.org/10.1016/j.scitotenv.2021.149310.

References

Almeida, S.M., Manousakas, M., Diapouli, E., Kertesz, Z., Samek, L., Hristova, E., Sega, K., Alvarez, R.P., Belis, C.A., Eleftheriadis, K., Group, K., Group I. E. R. S., 2020. Ambient particulate matter source apportionment using receptor modelling in European and Central Asia urban areas. Environ. Pollut. 266, 115199. https://doi.org/10.1016/j.envpol.2020.115199.

An, Z., Huang, R., Zhang, R., Tie, X., Li, G., Cao, J., Zhou, W., Shi, Z., Han, Y., Gu, Z., Ji, Y., 2019. Severe haze in northern China: a synergy of anthropogenic emissions and atmospheric processes. Proc. Natl. Acad. Sci. U. S. A. 116, 8657–8666. https://doi.org/10.1073/pnas.1900125116.

Barraza, F., Lambert, F., Jorquera, H., Villalobos, A.M., Gallardo, L., 2017. Temporal evolution of main ambient PM2.?5 sources in Santiago, Chile, from 1998 to 2012. Atmos. Chem. Phys. 17, 10093–10107. https://doi.org/10.5194/acp-17-10093-2017.

Bi, X., Dai, Q., Wu, J., Zhang, Q., Zhang, W., Luo, R., Cheng, Y., Zhang, J., Wang, L., Yu, Z., Zhang, Y., Tian, Y., Feng, Y., 2019. Characteristics of the main primary source profiles of particulate matter across China from 1987 to 2017. Atmos. Chem. Phys. 19, 3223–3243. https://doi.org/10.5194/acp-19-3223-2019.

Bie, S., Yang, L., Zhang, Y., Huang, Q., Li, J., Zhao, T., Zhang, X., Wang, P., Wang, W., 2021. Source appointment of PM2.5 in Qingdao port, east of China. Sci. Total Environ. 755, 142456. https://doi.org/10.1016/j.scitotenv.2020.142456.

Briggs, N.L., Long, C.M., 2016. Critical review of black carbon and elemental carbon source apportionment in Europe and the United States. Atmos. Environ. 144, 409–427. https://doi.org/10.1016/j.atmosenv.2016.09.002.

Brown, S.G., Eberly, S., Paatero, P., Norris, G.A., 2015. Methods for estimating uncertainty in PMF solutions: examples with ambient air and water quality data and guidance on

reporting PMF results. Sci. Total Environ. 518–519, 626–635. https://doi.org/10.1016/j.scitotenv.2015.01.022.
Chang, Y., Zou, Z., Deng, C., Huang, K., Collett, J., Lin, J., Zhuang, G., 2016. The importance of vehicle emissions as a source of atmospheric ammonia in the megacity of Shanghai. Atmos. Chem. Phys. 16, 3577–3594. https://doi.org/10.5194/acp-16-3577-2016.
Chen, Y., Xie, S., Luo, B., Zhai, C., 2017. Particulate pollution in urban Chongqing of Southwest China: historical trends of variation, chemical characteristics and source apportionment. Sci. Total Environ. 584–585, 523–534. https://doi.org/10.1016/j.scitotenv.2017.01.060.
Chen, Z., Chen, D., Wen, W., Zhuang, Y., Kwan, M.-P., Chen, B., Zhao, B., Yang, L., Gao, B., Li, R., Xu, B., 2019. Evaluating the "2 26" regional strategy for air quality improvement during two air pollution alerts in Beijing: variations in PM2.5 concentrations, source apportionment, and the relative contribution of local emission and regional transport. Atmos. Chem. Phys. 19, 6879–6891. https://doi.org/10.5194/acp-19-6879-2019.
Chow, J.C., Lowenthal, D.H., Chen, L.W.A., Wang, X., Watson, J.G., 2015. Mass reconstruction methods for PM2.5: a review. Air Qual. Atmos. Health 8, 243–263. https://doi.org/10.1007/s11869-015-0338-3.
Cui, Y., Cao, W., Ji, D., Gao, W., Wang, Y., 2021. Estimated contribution of vehicular emissions to carbonaceous aerosols in urban Beijing, China. Atmos. Res. 248, 105153. https://doi.org/10.1016/j.atmosres.2020.105153.
Daellenbach, K.R., Uzu, G., Jiang, J., Cassagnes, L.E., Leni, Z., Vlachou, A., Stefenelli, G., Canonaco, F., Weber, S., Segers, A., Kuenen, J.J.P., Schaap, M., Favez, O., Albinet, A., Aksoyoglu, S., Dommen, J., Baltensperger, U., Geiser, M., El Haddad, I., Jaffrezo, J.L., Prevot, A.S.H., 2020. Sources of particulate-matter air pollution and its oxidative potential in Europe. Nature 587, 414–419. https://doi.org/10.1038/s41586-020-2902-8.
Du, T., Wang, M., Guan, X., Zhang, M., Zeng, H.Y., Chang, Y., Zhang, L., Tian, P.F., Shi, J.S., Tang, C.G., 2020. Characteristics and formation mechanisms of winter particulate pollution in Lanzhou, Northwest China. J. Geophys. Res.-Atmos. 125. https://doi.org/10.1029/2020JD033369 e2020JD033369.
Esmaeilirad, S., Lai, A., Abbaszade, G., Schnelle-Kreis, J., Zimmermann, R., Uzu, G., Daellenbach, K., Canonaco, F., Hassankhany, H., Arhami, M., Baltensperger, U., Prevot, A.S.H., Schauer, J.J., Jaffrezo, J.L., Hosseini, V., El Haddad, I., 2020. Source apportionment of fine particulate matter in a middle eastern Metropolis, Tehran-Iran, using PMF with organic and inorganic markers. Sci. Total Environ. 705, 135330. https://doi.org/10.1016/j.scitotenv.2019.135330.
Gautam, S., Yan, F., Kang, S., Han, X., Neupane, B., Chen, P., Hu, Z., Sillanpaa, M., Li, C., 2020. Black carbon in surface soil of the Himalayas and tibetan plateau and its contribution to total black carbon deposition at glacial region. Environ. Sci. Pollut. Res. Int. 27, 2670–2676. https://doi.org/10.1007/s11356-019-07121-7.
Guan, X., Wang, M., Du, T., Tian, P., Zhang, N., Shi, J., Chang, Y., Zhang, L., Zhang, M., Song, X., Sun, Y., 2021. Wintertime aerosol optical properties in Lanzhou, Northwest China: emphasis on the rapid increase of aerosol absorption under high particulate pollution. Atmos. Environ. 246, 118081. https://doi.org/10.1016/j.atmosenv.2020.118081.
Henry, R.C., 2003. Multivariate receptor modeling by N-dimensional edge detection. Chemom. Intell. Lab. Syst. 65, 179–189. https://doi.org/10.1016/S0169-7439(02)00108-9.
Huang, F., Zhou, J., Chen, N., Li, Y., Li, K., Wu, S., 2019. Chemical characteristics and source apportionment of PM2.5 in Wuhan, China. J. Atmos. Chem. 76, 245–262. https://doi.org/10.1007/s10874-019-09395-0.
Huang, R., Zhang, Y., Bozzetti, C., Ho, K., Cao, J., Han, Y., Daellenbach, K.R., Slowik, J.G., Platt, S.M., Canonaco, F., Zotter, P., Wolf, R., Pieber, S.M., Bruns, E.A., Crippa, M., Ciarelli, G., Piazzalunga, A., Schwikowski, M., Abbaszade, G., Schnelle-Kreis, J., Zimmermann, R., An, Z., Szidat, S., Baltensperger, U., El Haddad, I., Prevot, A.S., 2014a. High secondary aerosol contribution to particulate pollution during haze events in China. Nature 514, 218–222. https://doi.org/10.1038/nature13774.
Huang, X., Bian, Q., Louie, P.K.K., Yu, J., 2014b. Contributions of vehicular carbonaceous aerosols to PM2.5 in a roadside environment in Hong Kong. Atmos. Chem. Phys. 14, 9279–9293. https://doi.org/10.5194/acp-14-9279-2014.
Huang, X., Liu, Z., Liu, J., Hu, B., Wen, T., Tang, G., Zhang, J., Wu, F., Ji, D., Wang, L., Wang, Y., 2017. Chemical characterization and source identification of PM2.5 at multiple sites in the Beijing–Tianjin–Hebei region, China. Atmos. Chem. Phys. 17, 12941–12962. https://doi.org/10.5194/acp-17-12941-2017.
Huang, Z., Huang, J., Bi, J., Wang, G., Wang, W., Fu, Q., Li, Z., Tsay, S.-C., Shi, J., 2010. Dust aerosol vertical structure measurements using three MPL lidars during 2008 China-U.S. joint dust field experiment. J. Geophys. Res., 115 https://doi.org/10.1029/2009jd013273.
Jain, S., Sharma, S.K., Vijayan, N., Mandal, T.K., 2020. Seasonal characteristics of aerosols (PM2.5 and PM10) and their source apportionment using PMF: a four year study over Delhi, India. Environ. Pollut. 262, 114337. https://doi.org/10.1016/j.envpol.2020.114337.
Ji, D., Cui, Y., Li, L., He, J., Wang, L., Zhang, H., Wang, W., Zhou, L., Maenhaut, W., Wen, T., Wang, Y., 2018. Characterization and source identification of fine particulate matter in urban Beijing during the 2015 spring festival. Sci. Total Environ. 628–629, 430–440. https://doi.org/10.1016/j.scitotenv.2018.01.304.
Juda-Rezler, K., Reizer, M., Maciejewska, K., Blaszczak, B., Klejnowski, K., 2020. Characterization of atmospheric PM2.5 sources at a central European urban background site. Sci. Total Environ. 713, 136729. https://doi.org/10.1016/j.scitotenv.2020.136729.
Karnae, S., John, K., 2011. Source apportionment of fine particulate matter measured in an industrialized coastal urban area of South Texas. Atmos. Environ. 45, 3769–3776. https://doi.org/10.1016/j.atmosenv.2011.04.040.
Kim, K.H., Kabir, E., Kabir, S., 2015. A review on the human health impact of airborne particulate matter. Environ. Int. 74, 136–143. https://doi.org/10.1016/j.envint.2014.10.005.
Lambe, A.T., Logue, J.M., Kreisberg, N.M., Hering, S.V., Worton, D.R., Goldstein, A.H., Donahue, N.M., Robinson, A.L., 2009. Apportioning black carbon to sources using highly time-resolved ambient measurements of organic molecular markers in Pittsburgh. Atmos. Environ. 43, 3941–3950. https://doi.org/10.1016/j.atmosenv.2009.04.057.
Lee, S., Liu, W., Wang, Y., Russell, A.G., Edgerton, E.S., 2008. Source apportionment of PM2.5: comparing PMF and CMB results for four ambient monitoring sites in the southeastern United States. Atmos. Environ. 42, 4126–4137. https://doi.org/10.1016/j.atmosenv.2008.01.025.
Lelieveld, J., Evans, J.S., Fnais, M., Giannadaki, D., Pozzer, A., 2015. The contribution of outdoor air pollution sources to premature mortality on a global scale. Nature 525, 367–371. https://doi.org/10.1038/nature15371.
Li, H., Wang, Q., Yang, M., Li, F., Wang, J., Sun, Y., Wang, C., Wu, H., Qian, X., 2016. Chemical characterization and source apportionment of PM2.5 aerosols in a megacity of Southeast China. Atmos. Res. 181, 288–299. https://doi.org/10.1016/j.atmosres.2016.07.005.
Li, Y., Liu, B., Xue, Z., Zhang, Y., Sun, X., Song, C., Dai, Q., Fu, R., Tai, Y., Gao, J., Zheng, Y., Feng, Y., 2020. Chemical characteristics and source apportionment of PM2.5 using PMF modelling coupled with 1-hr resolution online air pollutant dataset for Linfen, China. Environ. Pollut. 263, 114532. https://doi.org/10.1016/j.envpol.2020.114532.
Liu, B., Yang, J., Yuan, J., Wang, J., Dai, Q., Li, T., Bi, X., Feng, Y., Xiao, Z., Zhang, Y., Xu, H., 2017. Source apportionment of atmospheric pollutants based on the online data by using PMF and ME2 models at a megacity, China. Atmos. Res. 185, 22–31. https://doi.org/10.1016/j.atmosres.2016.10.023.
Malm, W.C., Sisler, J.F., Huffman, D., Eldred, R.A., Cahill, T.A., 1994. Spatial and seasonal trends in particle concentration and optical extinction in the United-States. J. Geophys. Res.-Atmos. 99, 1347–1370. https://doi.org/10.1029/93jd02916.
Manousakas, M., Papaefthymiou, H., Diapouli, E., Migliori, A., Karydas, A.G., Bogdanovic-Radovic, I., Eleftheriadis, K., 2017. Assessment of PM2.5 sources and their corresponding level of uncertainty in a coastal urban area using EPA PMF 5.0 enhanced diagnostics. Sci. Total Environ. 574, 155–164. https://doi.org/10.1016/j.scitotenv.2016.09.047.
Martínez-Cinco, M., Santos-Guzman, J., Mejia-Velazquez, G., 2016. Source apportionment of PM2.5 for supporting control strategies in the Monterrey Metropolitan Area, Mexico. J. Air Waste Manage. Assoc. 66, 631–642. https://doi.org/10.1080/10962247.2016.1159259.
Mooibroek, D., Schaap, M., Weijers, E.P., Hoogerbrugge, R., 2011. Source apportionment and spatial variability of PM2.5 using measurements at five sites in the Netherlands. Atmos. Environ. 45, 4180–4191. https://doi.org/10.1016/j.atmosenv.2011.05.017.
Norris, G., Duvall, R., Brown, S., Bai, S., 2014. EPA Positive Matrix Factorization (PMF) 5.0 Fundamentals and User Guide. U.S. Environmental Protection Agency, Washington, DC EPA/600/R-14/108 (NTIS PB2015-105147).
Paatero, P., Tapper, U., 1994. Positive matrix factorization: a non-negative factor model with optimal utilization of error estimates of data values. Environmetrics 5, 111–126. https://doi.org/10.1002/env.3170050203.
Qian, Z., Zhang, J., Wei, F., Wilson, W.E., Chapman, R.S., 2001. Long-term ambient air pollution levels in four chinese cities: inter-city and intra-city concentration gradients for epidemiological studies. J. Expo. Anal. Environ. Epidemiol. 11, 341–351. https://doi.org/10.1038/sj.jea.7500170.
Qiu, X., Duan, L., Gao, J., Wang, S., Chai, F., Hu, J., Zhang, J., Yun, Y., 2016. Chemical composition and source apportionment of PM10 and PM2.5 in different functional areas of Lanzhou, China. J. Environ. Sci. (China) 40, 75–83. https://doi.org/10.1016/j.jes.2015.10.021.
Resitoglu, I.A., Altinisik, K., Keskin, A., 2015. The pollutant emissions from diesel-engine vehicles and exhaust aftertreatment systems. Clean Techn. Environ. Policy 17, 15–27. https://doi.org/10.1007/s10098-014-0793-9.
Saraga, D., Maggos, T., Degrendele, C., Klanova, J., Horvat, M., Kocman, D., Kanduc, T., Garcia Dos Santos, S., Franco, R., Gomez, P.M., Manousakas, M., Bairachtari, K., Eleftheriadis, K., Kermenidou, M., Karakitsios, S., Gotti, A., Sarigiannis, D., 2021. Multi-city comparative PM2.5 source apportionment for fifteen sites in Europe: the ICARUS project. Sci. Total Environ. 751, 141855. https://doi.org/10.1016/j.scitotenv.2020.141855.
Saraga, D.E., Tolis, E.I., Maggos, T., Vasilakos, C., Bartzis, J.G., 2019. PM2.5 source apportionment for the port city of Thessaloniki, Greece. Sci. Total Environ. 650, 2337–2354. https://doi.org/10.1016/j.scitotenv.2018.09.250.
Schmidt, M.W.I., Noack, A.G., 2000. Black carbon in soils and sediments: analysis, distribution, implications, and current challenges. Glob. Biogeochem. Cycles 14, 777–793. https://doi.org/10.1029/1999gb001208.
Sowlat, M.H., Hasheminassab, S., Sioutas, C., 2016. Source apportionment of ambient particle number concentrations in Central Los Angeles using positive matrix factorization (PMF). Atmos. Chem. Phys. 16, 4849–4866. https://doi.org/10.5194/acp-16-4849-2016.
Su, C., Peng, X., Huang, X., Zeng, L., Cao, L., Tang, M., Chen, Y., Zhu, B., Wang, Y., He, L., 2020. Development and application of a mass closure PM2.5; composition online monitoring system. Atmos. Meas. Tech. 13, 5407–5422. https://doi.org/10.5194/amt-13-5407-2020.
Tan, J., Zhang, L., Zhou, X., Duan, J., Li, Y., Hu, J., He, K., 2017. Chemical characteristics and source apportionment of PM2.5 in Lanzhou, China. Sci. Total Environ. 601–602, 1743–1752. https://doi.org/10.1016/j.scitotenv.2017.06.050.
Tao, J., Gao, J., Zhang, L., Zhang, R., Che, H., Zhang, Z., Lin, Z., Jing, J., Cao, J., Hsu, S.C., 2014. PM2.5 pollution in a megacity of Southwest China: source apportionment and implication. Atmos. Chem. Phys. 14, 8679–8699. https://doi.org/10.5194/acp-14-8679-2014.
Thurston, G.D., Ito, K., Lall, R., 1994. A source apportionment of U.S. fine particulate matter air pollution. Atmos. Environ. 2011 (45), 3924–3936. https://doi.org/10.1016/j.atmosenv.2011.04.070.
Tian, P., Cao, X., Zhang, L., Wang, H., Shi, J., Huang, Z., Zhou, T., Liu, H., 2015. Observation and simulation study of atmospheric aerosol nonsphericity over the loess plateau in Northwest China. Atmos. Environ. 117, 212–219. https://doi.org/10.1016/j.atmosenv.2015.07.020.
Tian, P., Zhang, L., Ma, J., Tang, K., Xu, L., Wang, Y., Cao, X., Liang, J., Ji, Y., Jiang, J., Yung, Y., Zhang, R., 2018. Radiative absorption enhancement of dust mixed with

anthropogenic pollution over East Asia. Atmos. Chem. Phys. 18, 7815–7825. https://doi.org/10.5194/acp-18-7815-2018.

Toils, E., Saraga, D., Ammari, G., Gkanas, E., Gougoulas, T., Papaioannou, C., Sarioglou, A., Kougioumtzidis, E., Skemperi, A., Bartzis, J., 2014. Chemical characterization of particulate matter (PM) and source apportionment study during winter and summer period for the city of Kozani, Greece. Open Chem. 12, 643–651. https://doi.org/10.2478/s11532-014-0531-5.

Tositti, L., Brattich, E., Masiol, M., Baldacci, D., Ceccato, D., Parmeggiani, S., Stracquadanio, M., Zappoli, S., 2014. Source apportionment of particulate matter in a large city of southeastern Po Valley (Bologna, Italy). Environ. Sci. Pollut. Res. 21, 872–890. https://doi.org/10.1007/s11356-013-1911-7.

Venkataraman, C., Habib, G., Eiguren-Fernandez, A., Miguel, A.H., Friedlander, S.K., 2005. Residential biofuels in South Asia: carbonaceous aerosol emissions and climate impacts. Science 307, 1454–1456. https://doi.org/10.1126/science.1104359.

Wang, G., Deng, J., Zhang, Y., Zhang, Q., Duan, L., Hao, J., Jiang, J., 2020. Air pollutant emissions from coal-fired power plants in China over the past two decades. Sci. Total Environ. 741, 140326. https://doi.org/10.1016/j.scitotenv.2020.140326.

Wang, G., Zhang, R., Gomez, M.E., Yang, L., Levy Zamora, M., Hu, M., Lin, Y., Peng, J., Guo, S., Meng, J., Li, J., Cheng, C., Hu, T., Ren, Y., Wang, Y., Gao, J., Cao, J., An, Z., Zhou, W., Li, G., Wang, J., Tian, P., Marrero-Ortiz, W., Secrest, J., Du, Z., Zheng, J., Shang, D., Zeng, L., Shao, M., Wang, W., Huang, Y., Wang, Y., Zhu, Y., Li, Y., Hu, J., Pan, B., Cai, L., Cheng, Y., Ji, Y., Zhang, F., Rosenfeld, D., Liss, P.S., Duce, R.A., Kolb, C.E., Molina, M.J., 2016a. Persistent sulfate formation from London fog to Chinese haze. Proc. Natl. Acad. Sci. 113, 13630. https://doi.org/10.1073/pnas.1616540113.

Wang, Q., Qiao, L., Zhou, M., Zhu, S., Griffith, S., Li, L., Yu, J., 2018. Source apportionment of PM2.5 using hourly measurements of elemental tracers and major constituents in an urban environment: investigation of time-resolution influence. J. Geophys. Res.-Atmos. 123, 5284–5300. https://doi.org/10.1029/2017jd027877.

Wang, Y., Jia, C., Tao, J., Zhang, L., Liang, X., Ma, J., Gao, H., Huang, T., Zhang, K., 2016b. Chemical characterization and source apportionment of PM2.5 in a semi-arid and petrochemical-industrialized city, Northwest China. Sci. Total Environ. 573, 1031–1040. https://doi.org/10.1016/j.scitotenv.2016.08.179.

Watson, J., Chow, J., Chen, L.W.A., Wang, X., 2012. Reformulation of PM2.5 Mass Reconstruction Assumptions for the San Joaquin Valley.

Wei, N., Xu, Z., Wang, G., Liu, W., Zhouga, D., Xiao, D., Yao, J., 2019. Source apportionment of carbonaceous aerosols during haze days in Shanghai based on dual carbon isotopes. J. Radioanal. Nucl. Chem. 321, 383–389. https://doi.org/10.1007/s10967-019-06609-3.

Wong, Y., Huang, X., Louie, P., Yu, A., Chan, D., Yu, J., 2020. Tracking separate contributions of diesel and gasoline vehicles to roadside PM2.5 through online monitoring of volatile organic compounds and PM2.5 organic and elemental carbon: a 6-year study in Hong Kong. Atmos. Chem. Phys. 20, 9871–9882. https://doi.org/10.5194/acp-20-9871-2020.

Xu, H., Xiao, Z., Chen, K., Tang, M., Zheng, N., Li, P., Yang, N., Yang, W., Deng, X., 2019. Spatial and temporal distribution, chemical characteristics, and sources of ambient particulate matter in the Beijing-Tianjin-Hebei region. Sci. Total Environ. 658, 280–293. https://doi.org/10.1016/j.scitotenv.2018.12.164.

Yin, J., Harrison, R.M., Chen, Q., Rutter, A., Schauer, J.J., 2010. Source apportionment of fine particles at urban background and rural sites in the UK atmosphere. Atmos. Environ. 44, 841–851. https://doi.org/10.1016/j.atmosenv.2009.11.026.

Yu, Y., He, S., Wu, X., Zhang, C., Yao, Y., Liao, H., Wang, Q., Xie, M., 2019. PM2.5 elements at an urban site in Yangtze River Delta, China: high time-resolved measurement and the application in source apportionment. Environ. Pollut. 253, 1089–1099. https://doi.org/10.1016/j.envpol.2019.07.096.

Zhang, M., Tian, P., Zeng, H., Wang, L., Liang, J., Cao, X., Zhang, L., 2021. A comparison of wintertime atmospheric boundary layer heights determined by tethered balloon soundings and Lidar at the site of SACOL. Remote Sens. 13. https://doi.org/10.3390/rs13091781.

Zhang, Q., Zheng, Y., Tong, D., Shao, M., Wang, S., Zhang, Y., Xu, X., Wang, J., He, H., Liu, W., Ding, Y., Lei, Y., Li, J., Wang, Z., Zhang, X., Wang, Y., Cheng, J., Liu, Y., Shi, Q., Yan, L., Geng, G., Hong, C., Li, M., Liu, F., Zheng, B., Cao, J., Ding, A., Gao, J., Fu, Q., Huo, J., Liu, B., Liu, Z., Yang, F., He, K., Hao, J., 2019. Drivers of improved PM2.5 air quality in China from 2013 to 2017. Proc. Natl. Acad. Sci. U. S. A. 116, 24463–24469. https://doi.org/10.1073/pnas.1907956116.

Zhang, R., Wang, G., Guo, S., Zamora, M.L., Ying, Q., Lin, Y., Wang, W., Hu, M., Wang, Y., 2015. Formation of urban fine particulate matter. Chem. Rev. 115, 3803–3855. https://doi.org/10.1021/acs.chemrev.5b00067.

Zhang, W., Liu, B., Zhang, Y., Li, Y., Sun, X., Gu, Y., Dai, C., Li, N., Song, C., Dai, Q., Han, Y., Feng, Y., 2020. A refined source apportionment study of atmospheric PM2.5 during winter heating period in Shijiazhuang, China, using a receptor model coupled with a source-oriented model. Atmos. Environ. 222, 117157. https://doi.org/10.1016/j.atmosenv.2019.117157.

Zhong, Y., Wang, X., Cheng, S., 2020. Characteristics and source apportionment of PM2.5 and O3 during winter of 2013 and 2018 in Beijing. Atmosphere 11. https://doi.org/10.3390/atmos11121324.

Zhu, Y., Huang, L., Li, J., Ying, Q., Zhang, H., Liu, X., Liao, H., Li, N., Liu, Z., Mao, Y., Fang, H., Hu, J., 2018. Sources of particulate matter in China: insights from source apportionment studies published in 1987–2017. Environ. Int. 115, 343–357. https://doi.org/10.1016/j.envint.2018.03.037.

Zong, Z., Wang, X., Tian, C., Chen, Y., Fu, S., Qu, L., Ji, L., Li, J., Zhang, G., 2018. PMF and PSCF based source apportionment of PM2.5 at a regional background site in North China. Atmos. Res. 203, 207–215. https://doi.org/10.1016/j.atmosres.2017.12.013.